IL-9 sensitizes human T_H2 cells to proinflammatory IL-18 signals in atopic dermatitis

Stefanie Schärli, MSc, Fabian Luther, PhD, Jeremy Di Domizio, PhD, Christina Hillig, MSc, Susanne Radonjic-Hoesli, MD, PhD, Kathrin Thormann, DNP, et al

GRAPHICAL ABSTRACT

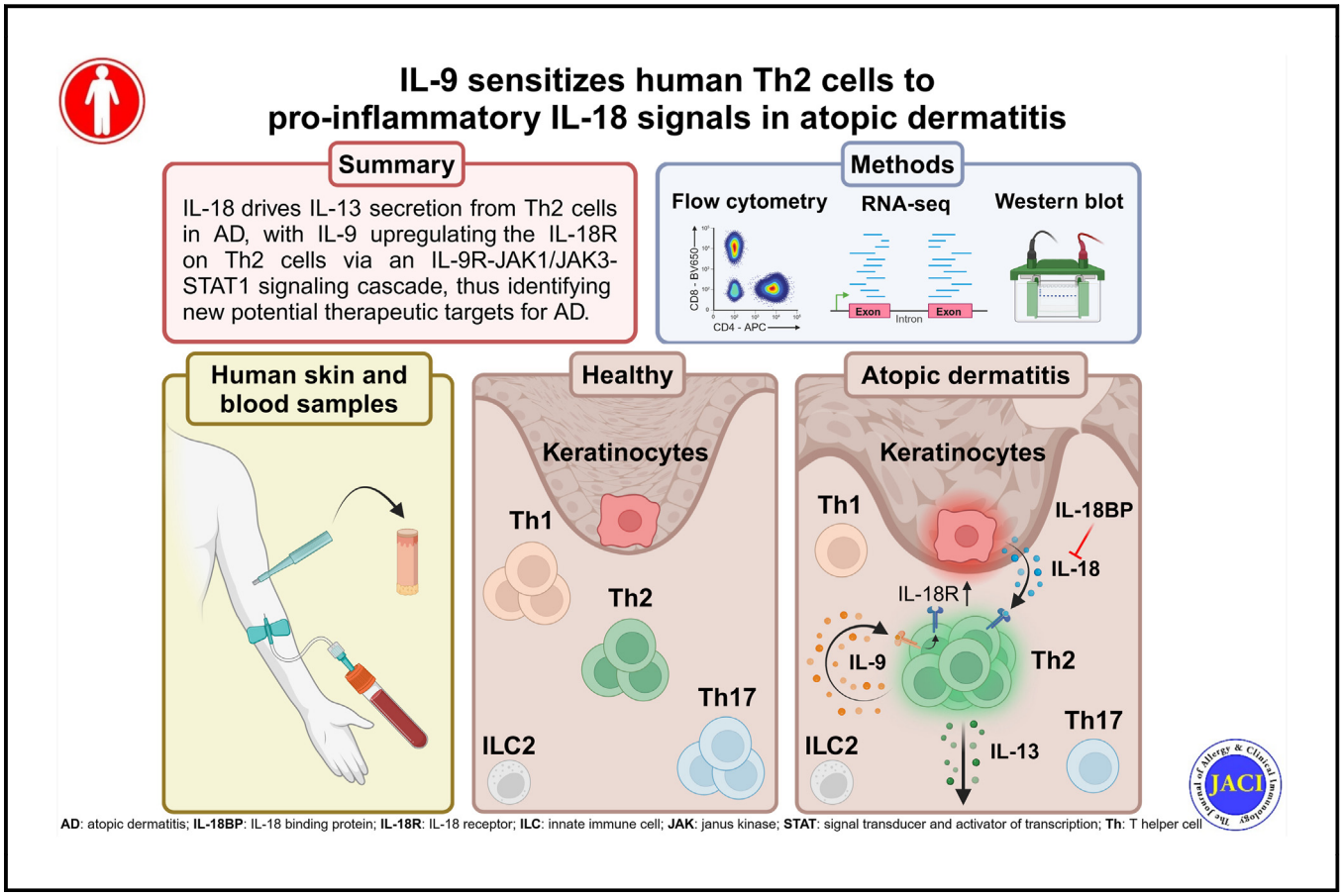

Capsule summary: IL-18 drives secretion of pathogenic cytokines from T_H2 cells in atopic dermatitis (AD), with IL-9 upregulating IL-18 receptor on T_H2 cells via an IL-9R–JAK1/JAK3-STAT1 signaling cascade, thus identifying new potential therapeutic targets for the treatment of AD.

J Allergy Clin Immunol 2025;155:491-513.

https://doi.org/10.1016/j.jaci.2024.10.027

IL-9 sensitizes human T_H2 cells to proinflammatory IL-18 signals in atopic dermatitis

Stefanie Schärli, MSc,[a] Fabian Luther, PhD,[a] Jeremy Di Domizio, PhD,[b] Christina Hillig, MSc,[c] Susanne Radonjic-Hoesli, MD, PhD,[a] Kathrin Thormann, DNP,[a] Dagmar Simon, MD,[a] Amalie Thorsti Møller Rønnstad, MD,[d] Iben Frier Ruge, MD,[d] Blaine G. Fritz, PhD,[e] Thomas Bjarnsholt, PhD, DMSc,[e,f] Angela Vallone, MSc,[a] Sanja Kezic, PhD,[g] Michael P. Menden, PhD,[c,h] Lennart M. Roesner, PhD,[i] Thomas Werfel, MD,[i] Jacob P. Thyssen, MD, PhD, DmSci,[d] Stefanie Eyerich, PhD,[j] Michel Gilliet, MD,[b] Nicole L. Bertschi, PhD,[a] and Christoph Schlapbach, MD, PhD[a] *Amsterdam, The Netherlands; Bern and Lausanne, Switzerland; Copenhagen, Denmark; Hannover and Munich, Germany; and Parkville, Australia*

Background: T_H2 cells crucially contribute to the pathogenesis of atopic dermatitis (AD) by secreting high levels of IL-13 and IL-22. Yet the upstream regulators that activate T_H2 cells in AD skin remain unclear. IL-18 is a putative upstream regulator of T_H2 cells because it is implicated in AD pathogenesis and has the capacity to activate T cells.

Objective: We sought to decipher the role of IL-18 in T_H2 responses in blood and skin of AD patients.

Methods: Peripheral blood mononuclear cells and skin biopsy samples from AD patients and healthy donors were used. Functional assays were performed *ex vivo* using stimulation or blocking experiments. Analysis was performed by flow cytometry, bead-based multiplex assays, RT-qPCR, RNA-Seq, Western blot, and spatial sequencing.

Results: IL-18Rα^+ T_H2 cells were enriched in blood and lesional skin of AD patients. Of all the cytokines for which T_H2 cells express the receptor, only IL-9 was able to induce IL-18R via an IL-9R–JAK1/JAK3-STAT1 signaling pathway. Functionally, stimulation of circulating T_H2 cells with IL-18 induced secretion of IL-13 and IL-22, an effect that was enhanced by costimulation with IL-9. Mechanistically, IL-18 induced T_H2 cytokines via activation of IRAK4, NF-κB, and AP-1 signaling in T_H2 cells, and neutralization of IL-18 inhibited these cytokines in cultured explants of AD skin lesions. Finally, IL-18 protein levels correlated positively with disease severity in lesional AD skin.

Conclusion: Our data identify a novel IL-9/IL-18 axis that contributes to T_H2 responses in AD. Our findings suggest that both IL-9 and IL-18 could represent upstream targets for future treatment of AD. (J Allergy Clin Immunol 2025;155:491-504.)

Key words: *Atopic dermatitis (AD), interleukin-9 (IL-9), IL-9 receptor (IL-9R), interleukin-18 (IL-18), interleukin-18 receptor (IL-18R), interleukin-1 receptor–associated kinase 4 (IRAK4), pathogenic T_H2 cells (pT_H2), upstream regulator of T_H2 cells*

Abbreviations used

AD:	Atopic dermatitis
AP-1:	Activator protein 1
APC:	Antigen-presenting cell
CRT_H2:	Chemoattractant receptor-homologous molecule expressed on T_H2 cells
DMSO:	Dimethyl sulfoxide
FACS:	Fluorescence-activated cell sorting
γc:	Common γ chain
HD:	Healthy donors
IL-18BP:	IL-18 binding protein
IL-18R:	IL-18 receptor
ILC2:	Group 2 innate lymphoid cells
IRAK4:	IL-1R–associated kinase 4
JAK:	Janus kinase
NF-κB:	Nuclear factor kappa–light-chain enhancer of activated B cells
PBMC:	Peripheral blood mononuclear cell
PSO:	Psoriasis
pT_H:	Pathogenic T helper
RNA-Seq:	RNA sequencing
RT-qPCR:	Real-time reverse transcription–quantitative PCR
STAT:	Signal transducer and activator of transcription
TCR:	T-cell receptor
TSLP:	Thymic stromal lymphopoietin
TYK2:	Tyrosine kinase 2

Atopic dermatitis (AD) is a common chronic inflammatory skin disease with a devastating impact on the quality of life of affected patients.[1,2] Although significant advancements have been made in the therapeutic landscape of AD, a significant

From [a]the Department of Dermatology, Inselspital, Bern University Hospital, Department for BioMedical Research (DBMR), University of Bern, Bern; [b]the Department of Dermatology, CHUV University Hospital, University of Lausanne, Lausanne; [c]the Computational Health Center, Institute of Computational Biology, Helmholtz Munich, Munich; [d]the Department of Dermatology, Bispebjerg Hospital, Copenhagen; [e]the Department of Immunology and Microbiology, University of Copenhagen, Copenhagen; [f]the Department of Clinical Microbiology, Copenhagen University Hospital, Rigshospitalet, Copenhagen; [g]the Department of Public and Occupational Health, Amsterdam University Medical Center, University of Amsterdam, Amsterdam Public Health Research Institute, Amsterdam; [h]the Department of Biochemistry and Pharmacology, Bio21 Molecular Science and Biotechnology Institute, The University of Melbourne, Parkville; [i]the Department of Dermatology and Allergy, Hannover Medical School (MHH), Hannover, Germany; and [j]the Center for Allergy and Environment (ZAUM), Technical University and Helmholtz Center Munich, Munich.

Received for publication June 27, 2024; revised September 28, 2024; accepted for publication October 23, 2024.

Available online November 7, 2024.

Corresponding author: Christoph Schlapbach, MD, PhD, Department of Dermatology, Inselspital, Bern University Hospital, University of Bern, Anna-Seiler-Allee 33, 3010 Bern, Switzerland. E-mail: christoph.schlapbach@insel.ch.

0091-6749

https://doi.org/10.1016/j.jaci.2024.10.027

proportion of patients remain with inadequately controlled disease, underscoring the need for novel treatment modalities.[3] This gap in effective management may be attributed to the complex nature of AD pathogenesis, which is dominated by the aberrant activation of T_H2 cells in lesional skin that secrete high levels of IL-13 and IL-22.[4,5] Yet the upstream regulators that activate T_H2 cells in human AD skin remain incompletely understood. Identifying proinflammatory upstream regulators of pathogenic T-cell populations holds the promise of uncovering novel therapeutic targets. In psoriasis (PSO), targeting IL-23 upstream of pT_H17 cells is more efficient and safer than neutralizing cytokines such as IL-17A downstream of both pathogenic and homeostatic T_H17 cells.[6,7] This clinical observation, together with a broad range of experimental findings,[8,9] suggests that IL-23–specific inhibition prevents the activation and maintenance of pT_H17 cells while allowing IL-23–independent production of IL-17A from homeostatic T_H17 cells to maintain epithelial barrier integrity.[7] This model helps explain why targeted IL-23 blockade is highly effective in PSO yet not associated with relevant cutaneous infections.[10] It is therefore tempting to speculate that targeting upstream activators of pT_H2 cells in a manner analogous to PSO may be highly efficient and safe for treating AD. As a consequence, identifying upstream cytokines that regulate T_H2 cell activation in AD is of utmost interest. Importantly, T_H2 cells with a "pathogenic" phenotype have been identified in a variety of atopic diseases, including AD, and termed "pathogenic" T_H2 cells because of their intricate link to disease pathogenesis. Such pT_H2 cells commonly express CRT_H2 (chemoattractant receptor-homologous molecule expressed on T_H2 cells), a G protein–coupled receptor that enables them to sense prostaglandin D_2, which further enhances their activation.[11]

In AD, IL-18 emerges as a promising candidate for the role as a proinflammatory upstream regulator of pathogenic T cells, as multiple lines of evidence link IL-18 to AD pathogenesis. First, gene variants close to the *IL18R1* gene are associated with AD risk.[12-14] Second, elevated IL-18 protein levels in skin of normal infants are strongly associated with the risk of developing severe AD within the first 2 years of life.[15] Third, IL-18 protein levels in both lesional and nonlesional skin and in serum correlate with disease severity of AD.[16-19] Fourth, IL-18 negatively affects skin barrier protein levels, including filaggrin, and individuals with filaggrin gene mutations and low natural moisturizing factor levels show increased expression of IL-18.[20-22] Fifth, mouse models show IL-18–dependent increase of signs and symptoms of AD-like skin inflammation.[23,24] Finally, murine group 2 innate lymphoid cells (ILC2s), the evolutionary precursors of T_H2 cells,[25] express the IL-18 receptor (IL-18R) specifically in skin, and secrete IL-13 after IL-18 stimulation.[26] Taken together, there is circumstantial and experimental evidence from both humans and mice to suggest a proinflammatory, disease-driving role of IL-18 in AD pathogenesis. However, the mechanisms by which IL-18 may promote type 2 inflammation in human AD remain poorly understood.

The IL-1 family member IL-18 is a potent proinflammatory cytokine that plays a crucial role in the host defense against infections by regulating both innate and acquired immune responses. IL-18 is constitutively expressed by various cell types as proIL-18, an inactive precursor.[17] In human skin, it is mainly produced by keratinocytes and, to a lesser degree, by antigen-presenting cells (APCs) such as Langerhans cells.[27,28] Upon inflammasome activation, proIL-18 is cleaved, leading to the secretion of mature IL-18.[29] Its biological activity is mediated through binding to the IL-18R, comprising the IL-18Rα chain (encoded by *IL18R1*) and the IL-18R accessory protein *(IL18RAP)*. Binding of IL-18 to IL-18R activates downstream signaling pathways involving key proteins such as IL-1 receptor–associated kinase 4 (IRAK4), nuclear factor kappa–light-chain enhancer of activated B cells (NF-κB), and activator protein 1 (AP-1).[30] In human skin, IL-18R is mainly expressed on T cells, Langerhans cells, and other APCs. The functional effect of IL-18 on its target cells is best studied in natural killer cells and T_H1 cells, in which IL-18 induces the production of large amounts of IFN-γ to promote a type 1 immune response.[17] However, its proinflammatory role in a prototypical T_H2-driven disease such as AD has remained a conundrum.[5]

Another cytokine whose role in AD remains unclear is IL-9. IL-9 belongs to the family of common γ chain (γc) cytokines and is linked to type 2 immunity and immunopathology.[31] In human skin, IL-9 is mainly secreted by recently activated T_H2 cells during early phases of allergic skin inflammation, where it has been shown to have auto- and paracrine proinflammatory functions.[32-34] While IL-9 has been shown to be increased in lesional skin and serum of AD patients,[35,36] its functional involvement in AD remains poorly defined.

To address this, and to shed light on the putative role of IL-18 as upstream regulator of T_H2 cells in AD, we analyzed the functional effect of IL-18 on T_H2 responses in blood and skin of AD patients. Given the well-established pathogenic function of T_H2 cytokines in AD, we focused our analysis on the ability of IL-18 to promote secretion of IL-13 and IL-22 from T_H2 cells. Although T_H22 cells are an important source of IL-22,[37] several studies, including single-cell RNA sequencing data from AD and other atopic diseases, indicate that T_H2 cells can also secrete significant amounts of IL-22.[4,38-41] We found that IL-18 indeed promotes T_H2 responses in AD patients and uncover a hitherto unidentified role for IL-9 in regulating the expression of IL-18R on T_H2 cells.

METHODS

Study design

This study aimed to investigate the functional role of IL-18 in the pathogenesis of AD. We used human peripheral blood mononuclear cells (PBMCs) from HD and AD patients as well as lesional AD skin biopsy samples to assess IL-18Rα expression and cytokine secretion in CRT_H2-expressing T_H cells by flow cytometry. Downstream target induction by IL-18 was investigated using *in vitro* primed T_H2 cells. The transcriptional profile of fluorescence-activated cell sorting (FACS)-sorted T_H2 clones incubated with IL-9 was analyzed by RNA sequencing (RNA-Seq) in order to evaluate the molecular signature of IL-9. To assess the mechanism by which IL-9 induces IL-18R, phosphorylation of downstream targets was measured in T_H2 clones by flow cytometry. Group sizes and numbers of repetitions are indicated in the figures.

Human blood was obtained from HD at the Swiss Blood Donation Center in Bern and used in compliance with the Federal Office of Public Health (authorization P_149). The study on human patient samples was approved by the medical ethics committee of the canton of Bern, Switzerland (no. 088/13; 2019-01068; 2019-00803). Written informed consent was obtained from all participants. Patient demographics are listed in Tables E1 and E2 in the Online Repository available at www.jacionline.org. Mechanistic studies were carried out using *in vitro* assays on

human tissue and blood samples, without implementing blinding or randomization.

Isolation of human PBMCs

Following the manufacturer's standard operating procedure, PBMC isolation using SepMate (STEMCELL Technologies) was used to isolate PBMCs.

Generation of *in vivo* primed T_H2 clones

$CD4^+$ T cells were isolated from PBMCs using the EasySep Human CD4 Positive Selection Kit II (catalog 17852, STEMCELL Technologies) as per the manufacturer's instructions. Individual memory T_H2 cell subsets were sorted with a purity of >90% according to the chemokine receptor expression $CXCR3^-CCR4^+CRT_H2^+$ or $CXCR3^-CCR4^+CCR8^+$ from $CD45RA^-CD25^-CD8^-CD3^+$ cells using MoFlow ASTRIOS with Summit 6.3.1 software (Beckman Coulter) into a 96-well plate. Individual cells were grown by periodic activation with phytohemagglutinin-L (1 μg/mL; 11249738001, Sigma-Aldrich) and irradiated allogeneic feeder cells (5×10^4 per well) in culture medium. Half of the nutrient medium for T-cell culture was replaced with fresh medium every second day, starting from day 2 after reactivation. T_H2 cell clones were analyzed in the resting state (≥14 days after the last expansion).

Generation of *in vitro* primed T_H2 cells

Human naive T cells were isolated from PBMCs using the EasySep Human Naïve $CD4^+$ T Cell Isolation Kit II (17555, STEMCELL Technologies) as per the manufacturer's instructions. Naive T cells were stimulated with αCD3/CD2/CD28 beads (T cell/bead = 2:1; 130-091-441, Miltenyi Biotec) and primed into T_H2 cells with IL-4 (50 ng/mL) (BioLegend). From cell culture initiation to analysis at day 25, the culture medium was supplemented with the indicated cytokines every other day. At day 10, T cells were polyclonally activated using ImmunoCult Human CD3/CD2/CD28 T Cell Activator (1:200; 10970, STEMCELL Technologies).

T-cell culture

T cells were cultured as previously described.[33] For inhibition of Janus kinase (JAK) 1 and JAK3, *in vivo* primed T_H2 clones were incubated with upadacitinib (50 nmol) or ritlecitinib (100 nmol), respectively, in either IL-2 (50 U/mL) and dimethyl sulfoxide (DMSO) alone or together with IL-9 (5 ng/mL). After 24 hours, IL-18Rα expression levels were measured by flow cytometry. For IRAK4, degradation, *in vitro* primed T_H2 cells were preincubated with either DMSO or KT-474 (SAR444656; 1 μmol). After 24 hours, KT-474 and DMSO were replenished, and IL-18 (100 ng/mL) was added. To assess IL-13 secretion, cell culture supernatants were collected and analyzed by LEGENDplex Human Th Cytokine Panel (12-plex) (741027, BioLegend) according to the manufacturer's instructions.

Isolation of human T cells from skin biopsy samples

Lesional skin biopsy samples were obtained from patients with AD. In order to assess IL-18Rα expression levels on CRT_H2^+ and CRT_H2^- T_H cells, the subcutaneous fat was removed. Subsequently, the sample was cut into 4 pieces and digested using the human Whole Skin Dissociation Kit (130-101-540, Miltenyi Biotec) according to manufacturer's protocol. After digestion, the tissue was cut into small pieces and passed through a 70 μm filter, followed by a 40 μm cell strainer. After centrifugation, flow cytometry was used to analyze the cells.

To investigate neutralization of IL-18 signaling, the subcutaneous fat of lesional AD skin biopsy samples was removed and the samples were quartered. Two nonadjecent quarters each were incubated in culture medium with or without IL-18 binding protein (IL-18BP; BioLegend). Cells that egressed from the sample were collected and analyzed by flow cytometry.

Flow cytometry

All antibodies used for flow cytometry are listed in Table E3 in the Online Repository available at www.jacionline.org. For surface staining, cell suspensions were incubated with antibodies in CellWASH (349524, BD Biosciences) at room temperature for 20 minutes. For intracellular detection of IRAK4 and phosphorylated STAT (signal transducer and activator of transcription) proteins, p65, and c-Jun, cells were fixed with fixation buffer (420801, BioLegend), permeabilized with True-Phos Perm Buffer (425401, BioLegend), and stained according to the manufacturer's instructions. To assess cytokine production, cell culture supernatants were collected and analyzed by the LEGENDplex Human Th Cytokine Panel (12-plex) (741027, BioLegend) or the human IL-13 Secretion Assay–Detection Kit (PE) (130-093-479, Miltenyi Biotec), and then cells were collected after treatment and labeled according to the manufacturer's instructions. Data were acquired on CytoFLEX (Beckman Coulter) and analyzed by CytExpert 2.5 (Beckman Coulter) or FlowJo 10.9.0 (Becton Dickinson) software.

Western blot analysis

All antibodies used for Western blot analysis are listed in Table E3. For the analysis of JAK1, JAK3, and tyrosine kinase 2 (TYK2) phosphorylation, 1×10^6 *in vivo* primed T_H2 clones were collected after treatment, washed with phosphate-buffered saline containing the Halt Protease and Phosphatase Inhibitor Cocktail (78446, Thermo Fisher Scientific), and lysed in 20 mmol Tris-HCl pH 7.5, 0.5% Nonidet P-40, 25 mmol NaCl, and 2.5 mmol EDTA containing the Halt Protease and Phosphatase Inhibitor Cocktail (78446, Thermo Fisher Scientific). Protein concentration was measured using the Pierce BCA protein assay kit (23227, Thermo Fisher Scientific). Sample loading buffer consisting of 62.5 mmol Tris-HCl (pH 6.8), 2% 2-mercaptoethanol, 2% SDS, 0.02% bromophenol blue, 14.8% glycerol, and 6 mol urea were added to the samples, and 7 μg of protein per lane were loaded onto a 10% SDS-PAGE gel. After electrophoresis (150 V, 45 minutes), proteins were transferred to a 0.45 μm Nitrocellulose Blotting membrane (GE10600002, Amersham Protran) by wet transfer (100 V, 75 minutes). Nonspecific sites were blocked for 1 hour with 5% nonfat milk in a TBS-T buffer (25 mmol Tris, pH 7.5, 150 mmol NaCl, and 0.1% Tween 20). Primary antibodies were incubated overnight at 4°C. Membranes were washed with the TBS-T buffer and incubated for 1 hour at room temperature with the corresponding secondary antibodies. Using Western Bright Quantum (K-12042-C20, Advansta) or SuperSignal West Atto Ultimate Sensitivity Substrate (A38556,

Thermo Fisher Scientific), the binding of specific antibodies was then visualized by Fusion Pulse TS and Evolution Capt Pulse 6 17.02 (Vilber) software.

RT-qPCR

For RT-qPCR (real-time reverse transcription–quantitative PCR), total RNA was isolated from cultured *in vitro*–primed T cells using the RNeasy Kit (74004, Qiagen) according to the manufacturer's instructions. Total mRNA quality was measured using the NanoDrop One/One Microvolume UV-Vis Spectrophotometer (701-058112, Thermo Fisher Scientific). The Omniscript RT Kit (205113, Qiagen) was used to generate complementary DNA. Real-time PCR was performed using TaqMan probe-based assays and measured using the 7300 Real-Time PCR System (Applied Biosystems; Thermo Fisher Scientific) and Sequence Detection 1.4 software. The expression of each ligand transcript was determined relative to the reference gene transcript (HPRT-1) and normalized to the expression of the target gene using the $2^{-\Delta\Delta Ct}$ method. Data are displayed as arbitrary relative units. All primers used are listed in Table E4 in the Online Repository available at www.jacionline.org.

Next-generation sequencing and data analysis

Five IL-9R$^+$ T$_H$2 clones isolated from blood and 3 IL-9R$^+$ T$_H$2 clones isolated from skin biopsy samples of HD were incubated in recombinant human IL-2 (5 U/mL) and in the presence or absence of recombinant human IL-9 (5 ng/mL) for 12 hours. The RNeasy Micro Kit (74004, Qiagen) was used for total RNA isolation according to manufacturer's instructions, and RNA-Seq was performed. The samples were submitted to the Next Generation Sequencing (NGS) Platform (Institute of Genetics, University of Bern). RNA integrity was analyzed by Qubit. For all samples, the RNA integrity number values were ≥8. The total RNA was transformed into a library of template molecules using TruSeq Stranded mRNA Sample Preparation Kits (Illumina) and the EpMotion 5075 (Eppendorf) robotic pipette system. Single-end 100 bp and paired-end 50 bp sequencing were performed using HiSeq3000 (Illumina). The RNA-Seq reads were mapped to the reference human genome (GRCh38, build 81) using the HISAT2 2.0.446 aligner.[42] HTseq-count 0.6.147 was used to count the number of reads per gene,[43] and the DESeq2 1.4.548 package[44] was used to test for differential expression between groups of samples. The RNA-Seq data are deposited on BioStudies (accession no. E-MTAB-12204). Table E5 in the Online Repository available at www.jacionline.org lists the recombinant proteins and chemicals used.

To investigate *IL18R1* expression in blood of PSO and blood and skin of AD patients, a publicly available single-cell RNA sequencing dataset (EGAS00001007055)[4] was reanalyzed by the Seurat 4.0 package.[45] The publicly available RNA-Seq dataset (GSE206391) was reanalyzed as previously described[46] to evaluate the spatial transcriptomic landscape of *IL18, IL13, IL18R1,* and *IL18RAP* in nonlesional and lesional PSO and AD skin.

Statistical analysis

GraphPad Prism 10.1.2 (GraphPad Software) was used for statistical analysis. Between-group comparisons were conducted with either a 1-way or 2-way ANOVA followed by pairwise comparisons for each group. To correct for multiple testing, the Dunnett, Tukey, or Šídák test was used. Matched samples were analyzed by 2-tailed paired *t* tests or repeated-measures ANOVA. The *n* values and corresponding statistical methods for individual experiments are indicated in figures. For all statistical analyses, a 95% confidence interval and $P < .05$ were considered significant.

Skin tape strip collection and measurement of protein concentrations

Skin tape strips were collected daily for 10 consecutive days using CuDerm D-squame tape strips mm in diameter (CuDerm). Eight tape strips were briefly applied to lesional AD skin with a standardized pressure (225 g/cm^2) for 10 seconds using a D-Squame pressure application pen. The tape was then removed with forceps, and a new tape was applied. The tapes were individually placed in sterile, nuclease-free tubes and stored at −80°C. The sixth tape was used for protein measurements, which were performed with a MSD Cytokine Multiplex kit (Meso Scale Diagnostics).

Spatial transcriptomics

Spatial transcriptomics was performed as previously described.[46]

RESULTS

T$_H$2 cells expressing IL-18Rα are present in AD

We first investigated whether T$_H$2 cells from blood and lesional skin of AD patients expressed IL-18R. We analyzed a published dataset where single-cell RNA and T-cell receptor (TCR) sequencing was applied on immune cells from skin biopsy samples and matched blood samples of AD and PSO patients.[4] Indeed, the AD-specific T$_H$2/T$_H$22 cell cluster (as defined by the authors)[4] had significantly upregulated *IL18R1* expression, whereas the PSO-specific T$_H$17/Tc17 cluster did not (Fig 1, *A* and *B*). When comparing TCR-identical T$_H$2 cell clones from blood and skin of individual AD patients, T$_H$2 cells in the skin showed upregulated *IL18R1* expression compared to their counterparts in the blood.[4] In addition, skin T$_H$2 cells also upregulated markers associated with pT$_H$2 cells, including *PTGDR2* (encoding CRT$_H$2), *IL17RB,* and *IL9R* (Fig 1, *C*).[11,47,48] We then confirmed increased IL-18Rα protein expression on CRT$_H$2$^+$ T$_H$2 cells in the blood of AD patients compared to healthy donors (HD) (Fig 1, *D,* and see Fig E1, *A,* in the Online Repository available at www.jacionline.org) and detected IL-18Rα-expressing CRT$_H$2$^+$ T$_H$2 cells in lesional skin of AD (Fig 1, *E,* and Fig E1, *B* and *C*). Taken together, these findings suggest that IL-18Rα$^+$ T$_H$2 cells are increased in blood and skin of AD patients and that T$_H$2 cells upregulate markers of pT$_H$2 cells when entering the skin in AD.

IL-9 induces IL-18Rα expression in IL-9R$^+$ T$_H$2 cells in synergy with IL-2

We next aimed at identifying the cytokine signals that induce IL-18R expression on pT$_H$2 cells. We stimulated T$_H$2 clones (selected for their phenotypic similarity to pT$_H$2 cells in terms of cytokine and cytokine receptor expression, as described previously[32,33]) with a selection of type 2 cytokines for which pT$_H$2 cells express the receptor, namely IL-2, IL-4, IL-7, IL-9, IL-15, IL-21, thymic stromal lymphopoietin (TSLP), TGF-β, and IL-25 (Fig 2, *A,* and see Fig E2, *A,* in the Online Repository available at www.jacionline.org).[11] Of all cytokines tested, only IL-9

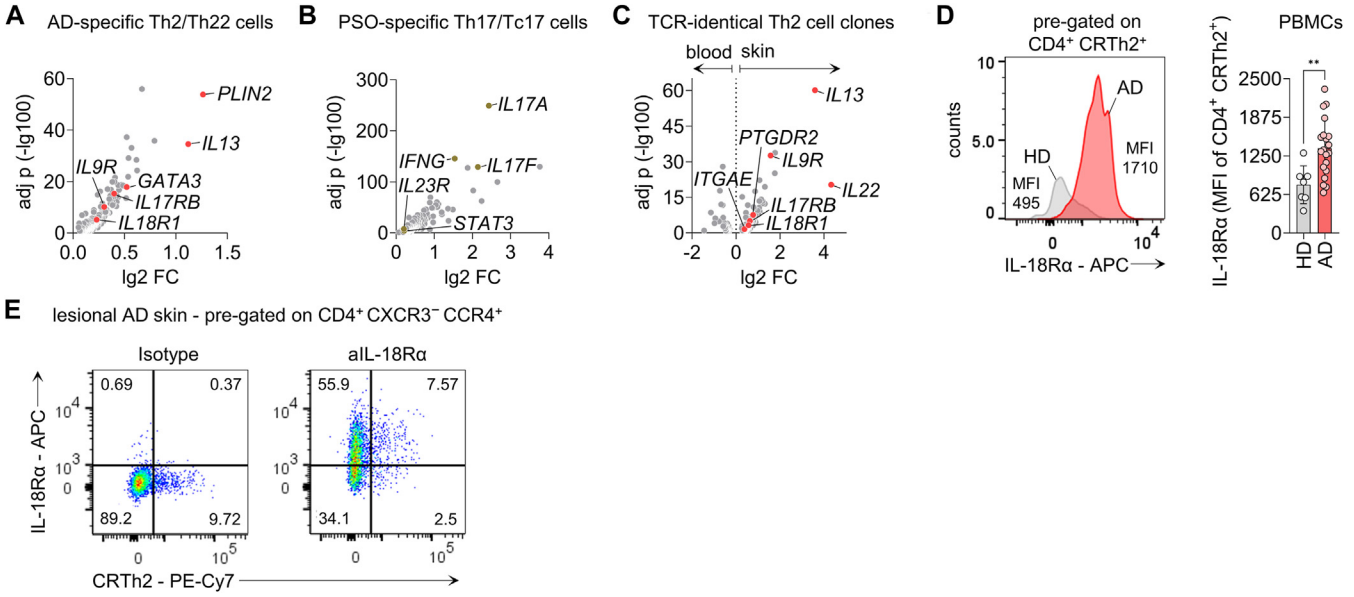

FIG 1. T_H2 cells expressing IL-18Rα are present in AD. (**A** and **B**) Volcano plot depicting significantly upregulated genes in AD-specific T_H2/T_H22 *(A)* and PSO-specific $T_H17/Tc17$ *(B)* cells isolated from blood comparing disease-specific T_H cell cluster and other $CD4^+$ T cells. **(C)** Volcano plot showing significantly differentially expressed genes of TCR-identical T_H2 cell clones between blood and skin of AD patients. **(D)** Representative histogram plot of 1 donor *(left)* and summary data of IL-18Rα expression on $CD4^+$ CRT_H2^+ cells isolated from PBMCs of HD or AD patients *(right)*. **(E)** Representative FACS plots of 1 donor displaying IL-18Rα and CRT_H2 expression on $CD4^+CXCR3^-CCR4^+$ T cells in lesional AD skin. Data are representative of independent experiments with 27 donors *(D)*. In *(A-C)*, differences between cell subsets were calculated as adjusted log fold change, and hypothesis testing was performed by Benjamini-Hochberg–adjusted *P* value (DESeq2). In *(D)*, statistical significance was determined by 2-tailed paired *t* test. Data are shown as means ± SDs. $*P < .05$, $**P < .01$, $***P < .001$, $****P < .0001$.

induced the expression of IL-18Rα in T_H2 cell clones, an effect that was enhanced by increased concentrations of IL-2 (Fig 2, *B,* and Fig E2, *C*). IL-9–induced IL-18Rα expression was dose- and time-dependent (Fig 2, *C,* and Fig E2, *D*) and relied on direct binding of IL-9 to its receptor, as evidenced by experiments with an IL-9R–blocking antibody (Fig 2, *D,* and Fig E2, *E*).

To verify the *in vivo* relevance of the above findings, we confirmed increased numbers of $CRT_H2^+/IL\text{-}9R^+$ pT_H2 cells in the peripheral blood of AD compared to HD patients (Fig 2, *E,* and see Fig E3, *A,* in the Online Repository available at www.jacionline.org). Characterization of the chemokine receptor profile of memory T_H cells revealed that IL-9R expression was significantly enriched in the $CXCR3^-/CCR4^+/CCR6^+/CRT_H2^+$ memory T_H cell population, confirming that IL-9R was preferentially expressed by pT_H2 cells (Fig 2, *F,* and Fig E3, *A* and *B*). IL-9 induced IL-18Rα expression in CRT_H2^+, but not CRT_H2^-, memory T_H2 cells from PBMCs of AD patients, as expected (Fig 2, *G,* and Fig E1, *A*).

Together, these data suggest that IL-9 is able to induce IL-18Rα expression on $IL\text{-}9R^+$ T_H2 cells and that a population of $CRT_H2^+/IL\text{-}9R^+/IL\text{-}18R\alpha^+$ pT_H2 cells is increased in AD patients.

IL-9 induces IL-18R expression in $IL\text{-}9R^+$ T_H2 cells via JAK1/JAK3-STAT1

We next investigated the mechanisms by which IL-9 induced IL-18Rα expression in T_H2 cells. First, the transcriptional response of T_H2 clones to IL-9 stimulation was measured by RNA-Seq. In line with our previous results, IL-9 induced expression of *IL18R1* and *IL18RAP,* but also, surprisingly, expression of type I IFN–stimulated genes such as *DTX3L, PARP9, STAT1,* and *IRF9* (Fig 3, *A*). This was not the result of secretion of IFN-I by T_H2 clones, as neither transcription nor secretion of IFN-I was observed after IL-9 stimulation (Fig E3, *C*). Given that the signaling events that lead to expression of type I IFN–stimulated genes typically involve signal transducer and activator of transcription 1 (STAT1),[49] we hypothesized that IL-9R was unique within the family of γc-cytokine receptors in its ability to induce signaling through STAT1. Indeed, among all γc-cytokines, only IL-9 induced phosphorylation of STAT1, while the other γc-cytokines variably induced pSTAT3, pSTAT5, and pSTAT6 (Fig 3, *B* and *C*), but not pSTAT1. Phosphorylation of STAT1 as a result of IL-9R signaling was confirmed in an independent experiment, showing that IL-9R signaling entails phosphorylation of STAT1, STAT3, and STAT5 (Fig 3, *D*). On the basis of the unexpected finding that IL-9R signaling activated pSTAT1, we investigated the signaling events upstream of STAT1. Because previous reports suggested association of TYK2 with IL-9R,[50] we investigated phosphorylation of all Janus kinase (JAK) family members downstream of IL-9R. We found phosphorylation of JAK1 and JAK3, but not TYK2, downstream of the activated IL-9R (Fig E3, *D*). In line with this, inhibition of JAK1 and JAK3 by upadacitinib or ritlecitinib, respectively, abrogated phosphorylation of STAT1 and upregulation of IL-18Rα by IL-9 (Fig 3, *E* and *F,* and see Fig E4, *A,* in the Online Repository available at www.jacionline.org).

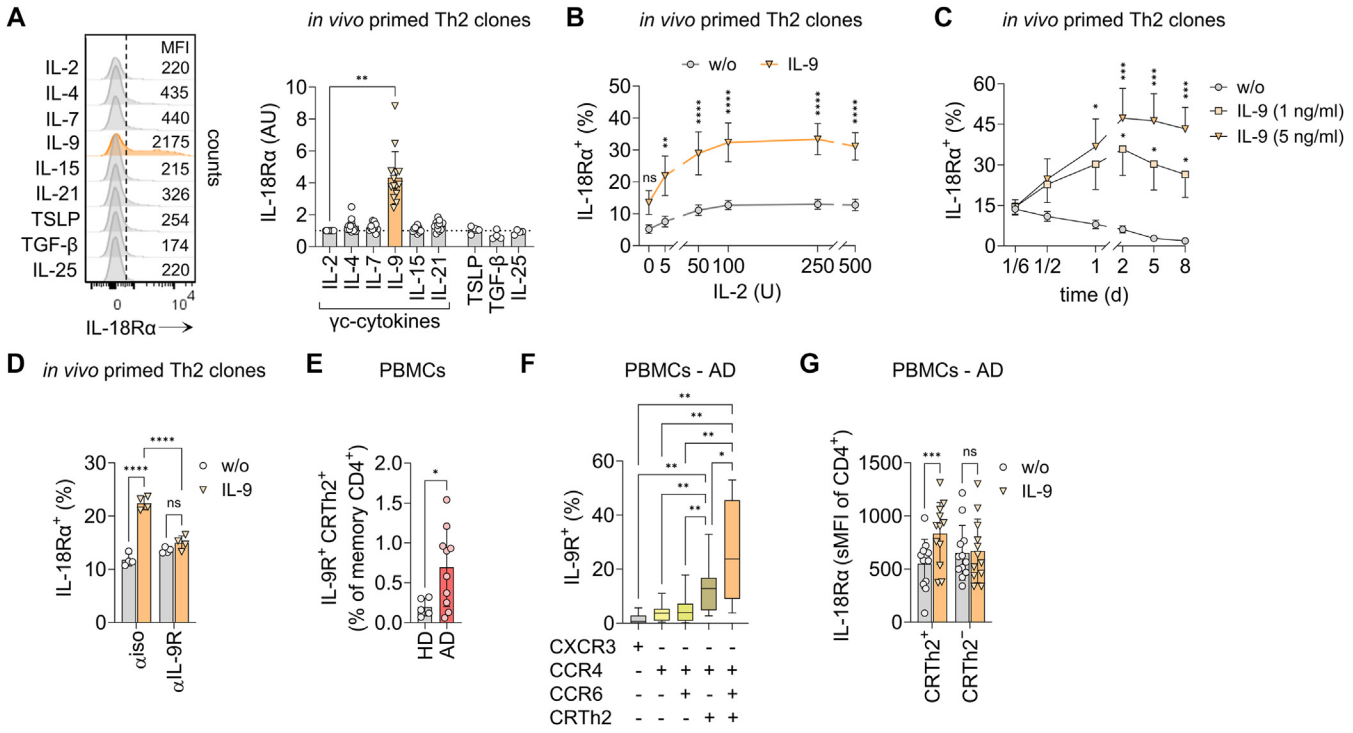

FIG 2. IL-9 induces IL-18Rα expression in IL-9R$^+$ T_H2 cells in synergy with IL-2. **(A)** Representative histogram plots of 1 donor *(left)* and summary data of IL-18Rα levels of *in vivo* primed T_H2 clones cultured in presence of either 1 γc-cytokine, IL-25, TSLP, or TGF-β *(right)*. **(B)** IL-18Rα levels of *in vivo* primed T_H2 clones cultured in different concentrations of IL-2 in presence or absence of IL-9. **(C)** Time course of IL-18Rα levels of *in vivo* primed T_H2 clones cultured in presence of IL-2 and different concentrations of IL-9. **(D)** *In vivo* primed T_H2 clones were preincubated for 1 hour with IL-9R–blocking antibody or isotype control, followed by incubation with IL-9 for 12 hours. IL-18Rα levels were measured by flow cytometry. **(E)** Frequency of IL-9R$^+$ CRT_H2^+ memory CD4$^+$ T cells isolated from PBMCs of healthy and AD donors. **(F)** IL-9R levels of memory CD4$^+$ T-cell subsets isolated from PBMCs of AD patients, stained for chemokine receptor profiles. **(G)** IL-18Rα levels of CRT_H2^+ and CRT_H2^- T_H cells of AD patients cultured in IL-9 for 16 hours. Data are representative of 1 experiment with 1 *(D)* or 3 (*B* and *C*) clones from 1 donor, or independent experiments with 10 clones from 2 different donors *(A)*, or 11 *(F)*, 12 *(G)*, or 15 *(E)* donors. Differences between cell subsets were calculated as 1-way ANOVA, followed by Dunnett test *(A)*, Tukey multiple comparisons tests *(F)*, or 2-way ANOVA, followed by Šídák multiple comparisons tests (*B-D* and *G*). In *(E)*, statistical significance was determined by 2-tailed paired *t* test. Data are shown as means ± SDs. **P* < .05, ***P* < .01, ****P* < .001, *****P* < .0001.

Together, these results indicate that IL-9 induces IL-18R expression in T_H2 cells through the activation of the JAK1/JAK3-STAT1 signaling cascade.

IL-9 enhances IL-18–induced IL-13 secretion from CRT_H2^+ T_H2 cells of AD patients

Having established the presence of IL-18Rα$^+$ T_H2 cells in AD and a role for IL-9 in the regulation of IL-18R expression, we next explored how the IL-9/IL-18 axis might contribute to AD pathogenesis. We focused our investigations on the ability of IL-18 to induce production of IL-13 and other T_H2 cytokines from T_H2 cells, given the well-established role of these cytokines in AD pathogenesis.[51,52] First, we stimulated *in vitro* primed T_H2 cells with IL-18 and found increased secretion of canonical T_H2 cytokines IL-5, IL-13, and IL-22 (Fig 4, *A, left*). The induction of IL-13 expression on IL-18 stimulation in *in vitro* primed T_H2 cells was validated by RT-qPCR (Fig 4, *A, right*). We next investigated the ability of IL-18, alone or in combination with IL-9, to induce IL-13 secretion in T_H2 cells from AD patients. While both IL-9 and IL-18 alone induced IL-13 secretion from CRT_H2^+ T_H2 cells, costimulation with IL-9 and IL-18 significantly enhanced their IL-13 secretion (Fig 4, *B, middle,* and Fig E1, *A*). This effect was not observed in CRT_H2^- T_H cells from AD patients (Fig 4, *B, right,* and Fig E4, *B, left*) or in CRT_H2^+ or CRT_H2^- T_H cells from HD (Fig 4, *C,* and Fig E4, *B, right*). This additive effect of IL-9 and IL-18 on IL-13 secretion is in line with our above findings and further suggests that IL-9 sensitizes CRT_H2^+ pT_H2 cells to respond to IL-18 in the setting of AD. However, stimulation of PBMCs from AD patients with IL-33 failed to induce IL-13 secretion from CRT_H2^+ T_H2 cells, whereas stimulation with IL-18 confirmed our previous results (Fig E4, *C*). We further validated the lack of IL-33R and IL-1RI expression on CRT_H2^+ T_H2 cells in a public RNA-Seq dataset (Fig E4, *D*).[48] These findings suggest that the increase in IL-13 production in T_H2 cells induced by IL-18 is not observed with other cytokines of the IL-1 family. Further, IL-18–induced secretion of IL-13 and IL-22 was confirmed by bead-based immunoassays of cell culture supernatants of PBMCs from AD patients (Fig 4, *D* and *E*).

In a next step, we investigated the signaling events engaged by IL-18 in human T_H2 cells. We assessed the phosphorylation of the NF-κB and the AP-1 pathway, which are known to be downstream

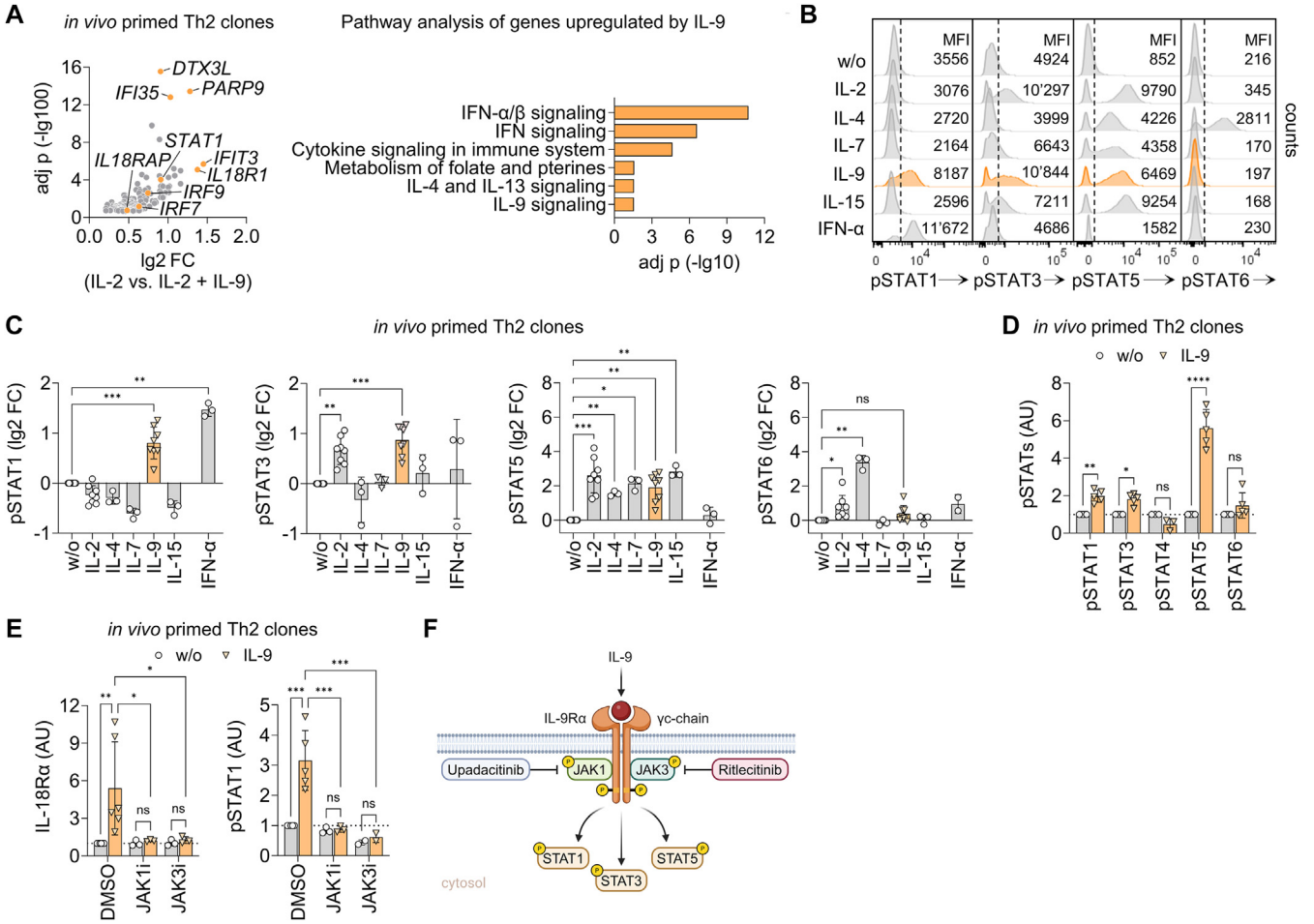

FIG 3. IL-9 induces IL-18R expression in IL-9R$^+$ T_H2 cells via JAK1/JAK3-STAT1. **(A)** Volcano plot depicting significantly upregulated genes in *in vivo* primed T_H2 clones isolated from blood and skin and cultured in presence of IL-2 and IL-9 for 12 hours *(left)* and corresponding pathway analysis *(right)*. (**B** and **C**) T_H2 clones were incubated with IL-2, IL-4, IL-7, IL-9, IL-15, or IFN-α for 15 minutes. Induction of pSTAT1, pSTAT3, pSTAT5, and pSTAT6 were measured by flow cytometry. Representative histogram plots of 1 donor are shown in *(B)* and summary data in *(C)*. **(D)** Phosphorylation of STAT1, STAT3, STAT4, STAT5, and STAT6 proteins in *in vivo* primed T_H2 clones on incubation with IL-9 for 15 minutes. **(E)** IL-18Rα expression *(left)* and pSTAT1 induction *(right)* in *in vivo* primed T_H2 clones on IL-9 stimulation in presence or absence of JAK1 inhibitor (JAK1i) upadacitinib and JAK3 inhibitor (JAK3i) ritlecitinib. **(F)** Schematic illustration of IL-9 signaling pathway and mechanism of used inhibitors. Data are representative of independent experiments with 5 (*D* and *E, right*) or 6 (*E, left*) clones from 2 donors, 8 (*C,* STAT6) or 9 (*C,* STAT1, STAT3, STAT5) clones from 4 donors, or 18 clones from 7 donors *(A)*. In *(A),* differences between cell subsets were calculated as adjusted log fold change, and hypothesis testing was performed by Benjamini-Hochberg–adjusted *P* value (DESeq2). Differences between groups were calculated as 1-way ANOVA followed by Dunnett multiple comparisons test *(C),* or as 2-way ANOVA followed by Šídák *(D)* or Tukey *(E)* multiple comparisons tests. Data are shown as means ± SDs. *$P < .05$, **$P < .01$, ***$P < .001$, ****$P < .0001$.

of the IL-18R.[30] IL-18 induced the phosphorylation of both p65 (NF-κB pathway) and c-Jun (AP-1 pathway); the former was phosphorylated rapidly and transiently, while the latter was phosphorylated slower and more steadily (Fig 4, *F*). Given the role of IRAK4 as key signaling molecule in the IL-18 signaling pathway[53] and the high expression of IRAK4 in T_H2 cells (Fig E4, *E*), we investigated IL-13 secretion on IL-18 stimulation in *in vitro* primed T_H2 cells in the presence of the IRAK4 degrader KT-474. We observed both degradation of IRAK4 and a reduction in IL-13 secretion in *in vitro* primed T_H2 cells after 24 hours of incubation with KT-474 (Fig 4, *G,* and Fig E4, *F*).

Given the importance of the NF-κB pathway for TCR signaling, we further investigated whether IL-18–induced NF-κB signals converge with those downstream of the TCR, thereby lowering the threshold of the TCR stimulus necessary for IL-13 secretion. Indeed, titration experiments with αCD3/CD2/CD28 showed that the presence of IL-18 lowered the threshold for submaximal IL-13 secretion (Fig E4, *G*).

These results, taken together, suggest a role of IL-18 as an upstream regulator of T_H2 cells, inducing IL-13 and IL-22 secretion in CRT$_H2^+$ T_H2 cells from AD patients via induction of the IRAK4, NF-κB, and AP-1 pathway. In this setting, IL-13

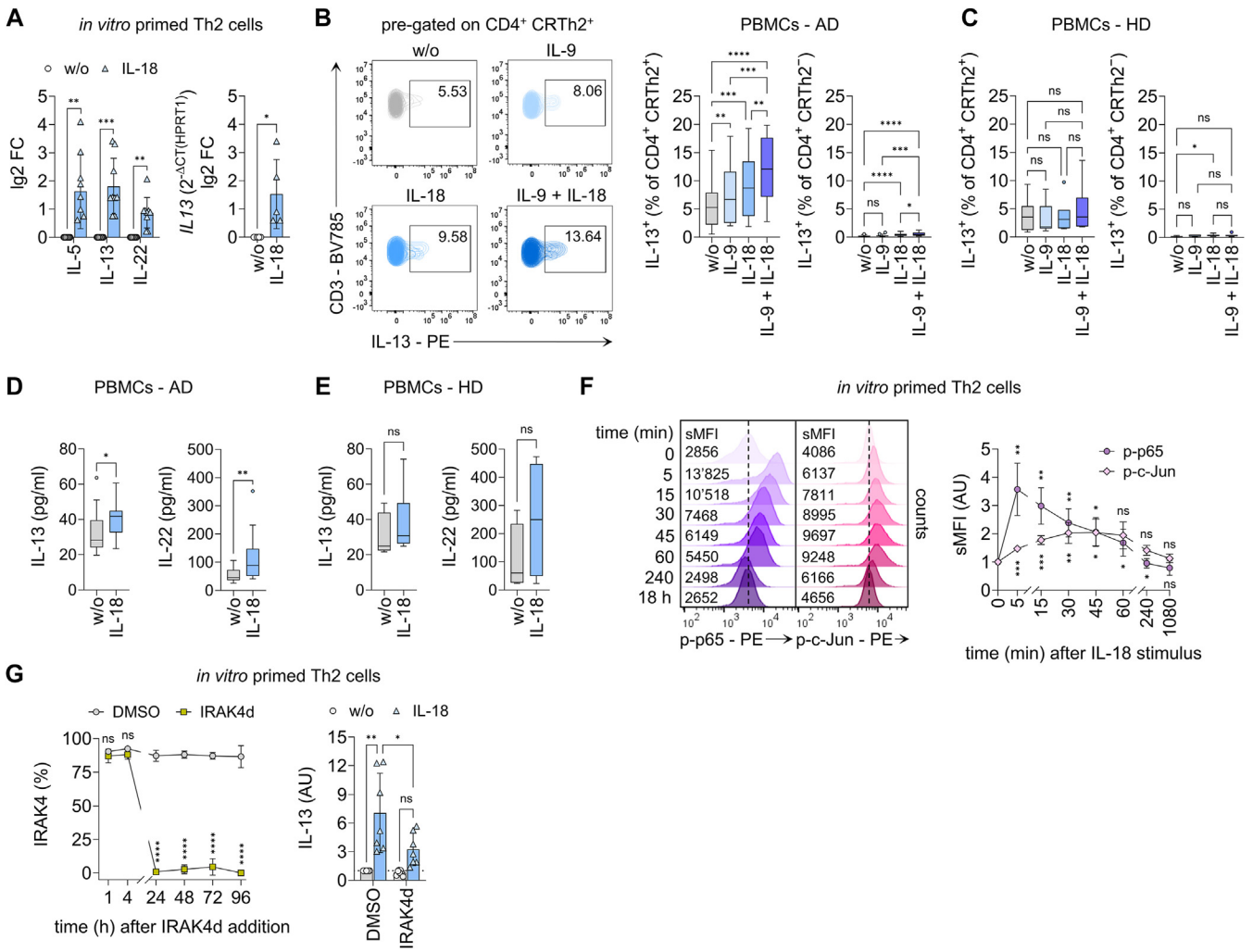

FIG 4. IL-9 enhances IL-18–induced IL-13 secretion from CRT_H2^+ T_H2 cells of AD patients. **(A)** Cytokine expression measured in cell culture supernatant *(left)* and *IL13* expression normalized to *HPRT1* analyzed by RT-qPCR *(right)* in *in vitro* primed T_H2 cells treated with IL-18 for 48 hours. (**B** and **C**) Representative FACS plots of 1 AD donor *(left)* and summary data of IL-13 secretion of $CD4^+CRT_H2^+$ and $CD4^+CRT_H2^-$ cells of PBMCs from AD donors *(B)* and HD *(C)*, incubated with IL-9 and/or IL-18 for 16 hours, and assessed by IL-13 Secretion Assay (Miltenyi Biotec) by flow cytometry *(right)*. (**D** and **E**) Cytokine expression of PBMCs isolated from AD patients *(D)* or HD *(E)* incubated with IL-18 for 16 hours, measured in cell culture supernatant by flow cytometry. **(F)** Representative histogram plots of 1 donor *(left)* and summary data of time course of phosphorylated p65 and c-Jun in *in vitro* primed T_H2 cells cultured in presence of IL-18 *(right)*. **(G)** Time course of IRAK4 *(left)* and IL-13 expression on IL-18 stimulation for 24 hours *(right)*, measured in cell culture supernatant, in *in vitro* primed T_H2 cells cultured in presence or absence of IRAK4 degrader (IRAK4d) KT-474 (SAR444656), assessed by flow cytometry. Data are representative of independent experiments with 2 *(G, left)*, 5 *(A, right)*, 6 (*E* and *F*), 7 (*C* and *G, right*), 8 *(A, left)*, 17 *(D)*, or 18 *(B)* donors. In (*B, C,* and *F*), differences between treatment groups were calculated as 2-way ANOVA, followed by Šídák (*F* and *G, left*), Tukey (*B* and *C*), or uncorrected Fisher LSD *(G, right)* multiple comparisons tests. In (*A, D,* and *E*), statistical significance was determined by 2-tailed paired *t* test. Data are shown as means ± SDs. $*P < .05$, $**P < .01$, $***P < .001$, $****P < .0001$.

production appears to be enhanced in the presence of IL-9 as a result of increased IL-18Rα expression on CRT_H2^+ T_H2 cells.

Neutralization of IL-18 in skin explants of AD inhibits IL-13 secretion from T_H2 cells

Having demonstrated that IL-18 promotes IL-13 secretion from circulating T_H2 cells in AD, we aimed at verifying our findings in explants of lesional AD skin. Indeed, blocking of IL-18 signaling by incubating skin explants with IL-18BP inhibited IL-13 and IL-22 secretion from lesional immune cells, as measured by bead-based immunoassays of the cell culture supernatant (Fig 5, *A* and *B*). Single-cell analysis of cells that egressed from skin explants showed that $CD4^+$ T_H cells were the main source of IL-13 in this *ex vivo* model and confirmed that incubation with IL-18BP specifically inhibited IL-13 secretion from CRT_H2^+ T_H2 cells, but not from CRT_H2^- $CD4^+$ T_H cells (Fig 5, *C,* and Fig E4, *H*).

Finally, we aimed at further substantiating a pathogenic involvement of IL-18 in AD lesions. For this purpose, we

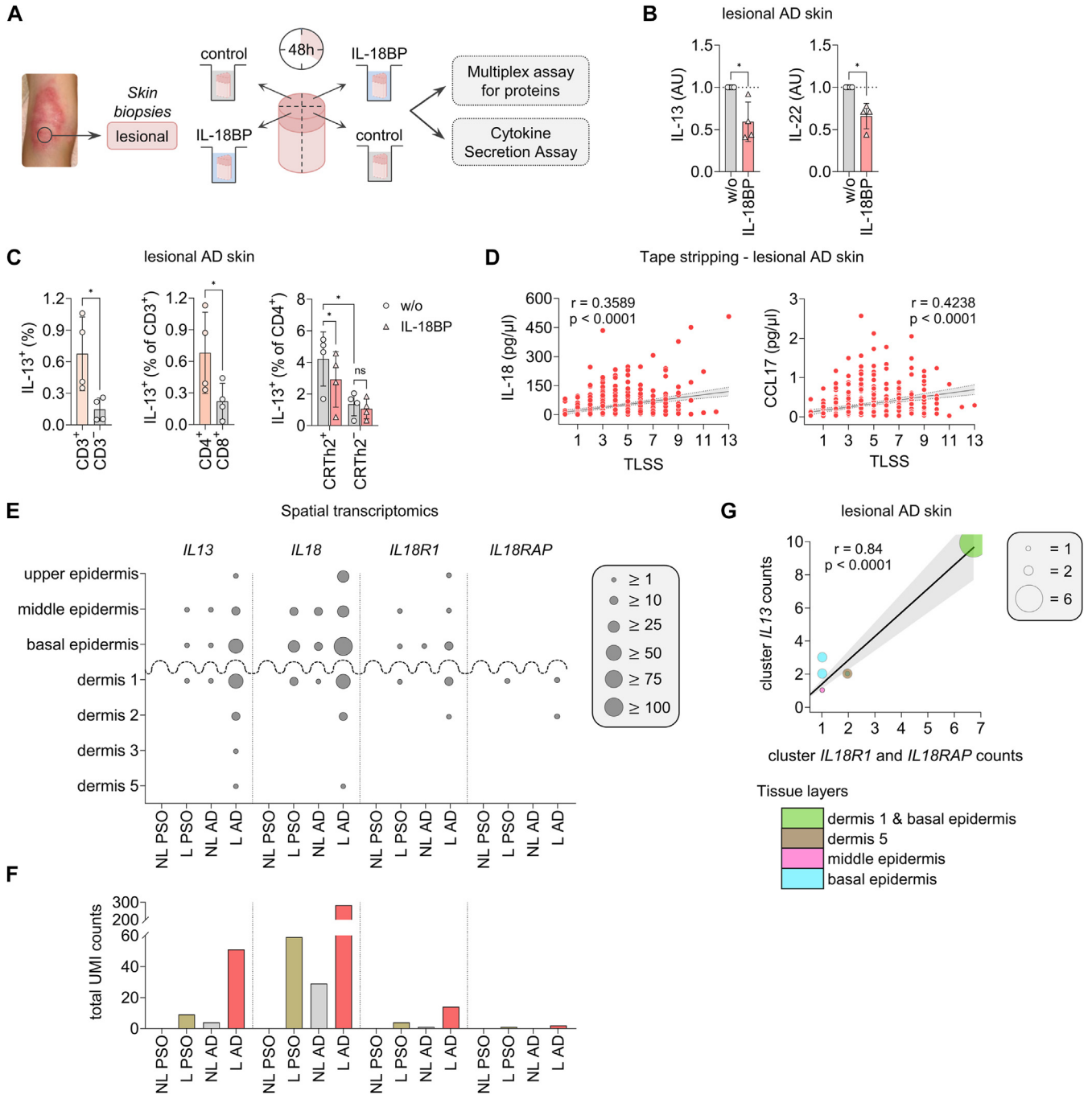

FIG 5. Neutralization of IL-18 in skin explants of AD inhibits IL-13 secretion from T_H2 cells. **(A)** Schematic illustration of experimental approach. **(B)** Cytokine expression of lesional AD skin biopsy samples incubated with IL-18BP for 48 hours, measured in cell culture supernatant by flow cytometry. **(C)** IL-13 secretion of egressed $CD3^+/CD3^-$ *(left)*, $CD4^+/CD8^+$ *(middle),* and CRT_H2^+/CRT_H2^- T_H *(right)* cells from lesional AD skin biopsy samples, incubated with IL-18BP for 48 hours, assessed by IL-13 Secretion Assay (Miltenyi Biotec) by flow cytometry. **(D)** In-sample correlations between IL-18 *(left)* and CCL17 *(right)* protein levels and TLSS in lesional skin of AD patients (n = 41). **(E)** Unique molecular identifier (UMI) counts of *IL13, IL18, IL18R1,* and *IL18RAP* expressed in manually annotated tissue layers "upper, middle, and basal epidermis" and "dermis depth 1, 2, 3, and 5" and corresponding total UMI counts **(F)** in nonlesional (NL) and lesional (L) skin of AD and PSO patients (n = 36). **(G)** Spatial weighted Spearman correlation indicating spatial relation of *IL13* and *IL18R1* and *IL18RAP* located in epidermis and dermis. Shown is radius 0 with highest correlation value. Each point represents a cluster of *IL13, IL18R1,* and *IL18RAP,* and size of each point indicates number of *IL13* transcripts in a cluster. Each spot's color corresponds to respective tissue layer. Data are representative of independent experiments with 4 donors (*B* and *C*). Statistical significance was determined by 2-tailed paired *t* test (*B* and *C, left, middle*), Spearman correlation *(D),* or ordinary least squares model *(G).* In *(C, right),* differences between treatment groups were calculated as 1-way ANOVA, followed by multiple comparisons test. Data are shown as means ± SDs. *Shaded areas* in *(D)* and *(G)* indicate 95% confidence intervals. **P* < .05, ***P* < .01, ****P* < .001, *****P* < .0001. *CCL17,* C-C motif chemokine ligand 17; *TLSS,* target lesion severity score.

correlated epidermal protein levels from lesional AD skin of young adults, as measured by multiplex immunoassays of skin tape strips, with the target lesion severity score.[54] Indeed, IL-18 protein levels correlated positively with AD severity (Spearman correlation coefficient $r = 0.3589$, $P < .0001$), thereby correlating to a similar degree with lesion severity as did CCL17 (C-C motif chemokine ligand 17; Spearman correlation coefficient $r = 0.4238$, $P < .0001$), a well-established biomarker of AD severity (Fig 5, *D*).[15,55,56] IL-13 protein levels were not measured above the level of detection, hence precluding correlation analysis with IL-18.

To gain insights into the spatial distribution of IL-18 and IL-18R expression in lesional AD skin, we reanalyzed a publicly available spatial sequencing dataset including nonlesional and lesional skin of PSO and AD patients. Transcripts of *IL13, IL18,* and *IL18R1* were readily detected in the epidermis and upper dermis of lesional AD skin, whereas nonlesional AD and lesional PSO skin showed markedly lower levels of these transcripts. No *IL13, IL18,* or *IL18R1* transcripts were detected in nonlesional PSO skin. *IL18RAP* was only detected at low levels in the upper dermal layers of lesional AD and, to a lesser degree, PSO skin, in line with the relatively low mRNA expression levels of *IL18RAP* in immune cells. Strikingly, the distribution of the *IL13, IL18,* and *IL18R1* transcripts showed a congruent pattern throughout all epidermal and upper dermal layers, suggesting coexpression of these transcripts in close spatial proximity (Fig 5, *E* and *F*). Indeed, spatial correlation between *IL13* and *IL18R1*/*IL18RAP* in the epidermis and dermis of lesional AD skin showed strong and significant correlation (considering their presence in the same spot; radius 0) (Fig 5, *G*).

Taken together, the above data support the presence of biologically active IL-18 in lesional AD skin and uncover its ability to promote the secretion of pathogenic cytokines such as IL-13 from IL-18Rα^+ T_H2 cells.

DISCUSSION

Our study assessed the functional role of IL-18 in the pathogenesis of AD by analyzing its ability to promote cytokine secretion from T_H2 cells. We found that functional IL-18Rα is expressed on CRT$_H2^+$ T_H2 cells in both blood and lesional skin of AD patients and that IL-9, in synergy with IL-2, upregulates its expression via binding to IL-9R. Stimulation of T_H2 cells with IL-18 induced secretion of IL-13, a well-established pathogenic cytokine in AD, and this effect was increased by costimulation with IL-9. Importantly, experiments with skin explants suggested that biologically active IL-18 is present in lesional AD skin and that blocking IL-18 in this context reduces the secretion of IL-13 from T_H2 cells. The only partial reduction of IL-13 and IL-22 secretion by IL-18BP indicates that pT_H2 cells might additionally be under the influence of other activating cytokines or that pT_H2 cells express certain levels of IL-13 and IL-22 independent of upstream activation.[1,2] When comparing AD to PSO, we did not detect upregulation of *IL18R1* expression in the PSO-specific T_H17/Tc17 cluster of PSO patients.[4] Furthermore, we detected lower *IL18* and *IL18R1* transcripts in lesional PSO skin, suggesting that IL-18 plays a specific role in AD.[46] Our data provide functional evidence that IL-18 plays a proinflammatory role in AD by inducing the secretion of pathogenic cytokines from T_H2 cells and uncover a role of IL-9 in the regulation of IL-18R expression on T_H2 cells.

Our findings add to a growing body of evidence linking IL-18 to AD pathogenesis and close an important knowledge gap by showing how this innate cytokine may promote T_H2-mediated skin inflammation. While IL-18 has been shown to promote both T_H1 and T_H2 cell responses depending on the inflammatory and genetic environment,[57] it has never been shown to directly promote secretion of pathogenic cytokines from T_H2 cells in AD patients. The implications of a putative IL-18/T_H2 axis driving AD are manifold.

The existence of an IL-18/T_H2 axis prompts the question of how proIL-18 might be activated and secreted from keratinocytes in AD. In this regard, *Staphylococcus aureus* has been demonstrated to activate the canonical NLRP1 inflammasome in keratinocytes, resulting in the secretion of active IL-18.[58] This establishes a direct connection between *S aureus,* a prevalent colonizer and pathogen in AD skin,[59] and the secretion of IL-18. In addition, IL-18 has also been identified as a target of the noncanonical inflammasome, wherein lipopolysaccharide-activated caspase-4/5 can directly process IL-18 during gram-negative bacterial infections.[60] Given that gram-negative bacteria are not associated with skin inflammation in AD,[61] it will be interesting to investigate whether there are lipopolysaccharide-independent activators of the noncanonical inflammasome that play a role in triggering IL-18 release in AD skin.

Our findings underscore the potential role of IL-18 as an upstream regulator of pT_H2 cells and as a drug target in AD. Several epithelial-derived cytokines and mediators have been proposed as upstream drivers in AD. These include prostaglandin D_2, TSLP, IL-1α, and IL-33.[1,2] However, clinical trials investigating inhibitors of these pathways in AD have all failed (NCT04988308),[62-65] leaving IL-18 as one of the few potential upstream regulators of T_H2 responses worth targeting. Notably, an anti–IL-18 antibody has shown promising efficacy in moderate-to-severe AD in a phase 1b study (NCT04975438) and is now being further developed. In addition to neutralizing IL-18 directly, blocking IL-18R signaling appears promising too. Inhibiting IRAK4 downstream of the IL-18R has indeed been shown to reverse pathogenic molecular signatures and improve clinical signs and symptoms of AD in early clinical trials.[53,66] Therefore, the promise of targeting upstream activators to reverse aberrant activation of T_H2 cells in AD skin might become a reality in the future.

Our study supports the complex role of IL-18 in mediating both T_H1 and T_H2 immune responses.[67] Traditionally, IL-18 has been viewed as a proinflammatory mediator initiating IFN-γ production in T_H1 and natural killer cells.[17] However, the effect of IL-18 on memory T_H cells appears to be context-dependent and predetermined by their polarization state. Our data, in conjunction with the current literature,[17] suggest that IL-18 will amplify cytokine expression according to the differentiation state of the target memory T cell—that is, it will induce IFN-γ production from T_H1 cells and IL-13 from T_H2 cells. In the T_H2-dominant environment of AD skin, IL-18 might thus induce IL-13 rather than IFN-γ. However, this hypothesis warrants further investigation to fully elucidate the dichotomous role of IL-18 in human skin inflammation.

The identification of IL-9 as a regulator of IL-18R expression on T_H2 cells suggests a novel role of this enigmatic cytokine in skin inflammation. Paracrine IL-9, coming from TCR-stimulated T_H2 cells in the context of acute skin inflammation,[32,68,69] may sensitize IL-9R$^+$ T_H2 cells to IL-18 signals, thereby promoting IL-13

secretion. Thus, IL-9R–expressing T_H2 cells might represent a tissue-resident T_H cell population poised to react to the tissue alarmin IL-18.[70] Interestingly, *IL9R* is among the most consistently expressed genes on pT_H2 cells from multiple atopic diseases including AD, further supporting a role of IL-9/IL-9R signaling in atopic diseases.[4,11] Moreover, our data propose that IL-9R is the only γc-receptor on T_H2 cells to signal through STAT1, which helps explain the unique ability of IL-9 to induce IL-18R expression. Although STAT1 activation via IL-9R has been reported previously in cancer cell lines and genetically modified T cells,[71,72] it has never been observed in primary human T_H cells. These findings have therapeutic implications, given the emergence of JAK inhibitors in clinical practice and the development of STAT1 degraders.[73-75]

Our study has a number of limitations and raises important questions that need to be addressed in future investigations. By focusing on T_H2 cells, we have not investigated the contribution of other IL-18R$^+$ cells in AD skin to the overall immune response to IL-18. Even though T_H2 cells can be viewed as a key node in AD pathogenesis,[5,39] a relevant contribution of additional IL-18–responsive immune cells cannot be ruled out, and this warrants further investigation. Notably, murine ILC2s have been identified as significant contributors to type 2 skin inflammation by several lines of evidence. First, the numbers of ILC2s are elevated in lesional AD skin and mouse models of AD-like inflammation. Second, they are preferentially activated by IL-18, resulting in the secretion of type 2 cytokines. Third, IL-18 deficiency results in attenuated AD-like skin inflammation in mice.[26] However, the role of ILC2s in human AD remains to be investigated.[76] Further, the need for concomitant TCR stimulation of IL-18–responsive T_H2 cells in AD remains largely unanswered. Whether IL-18 modulates the response of antigen-stimulated T_H2 cells or whether IL-18 might activate T_H2 cells in the absence of cognate antigen, possibly in conjunction with additional nonspecific T-cell–extrinsic factors, requires further investigations. Finally, we have not investigated the role of IL-37 and IL-18BP, two naturally expressed modulators of IL-18 activity, in our study.[17] In view of their potent immunomodulatory function, further research is required to understand the intricate relationship between IL-18, IL-37, and IL-18BP in AD.

Despite these limitations, our data provide new insights into the role of IL-18 in AD pathogenesis and uncover a role for IL-9 in regulating IL-18R expression on T_H2 cells. This has important implications for the development of novel therapeutics for AD that target upstream activators of pT_H2 cells.

DISCLOSURE STATEMENT

Supported by the Swiss National Science Foundation (grant 320030_192479), Bern Center for Precision Medicine (pilot project grant), Ruth & Arthur Scherbarth Foundation (project grant) (all to C.Sc.), the SKINTEGRITY.CH collaborative research project (S.S., F.L., J.D.D., M.G., N.L.B., and C.Sc.), the Deutsche Forschungsgemeinschaft through TUM International Graduate School of Science and Engineering (IGSSE) (C.H., M.P.M., and S.E.), and the Bio21 Molecular Science and Biotechnology Institute (M.P.M.).

Disclosure of potential conflict of interest: L. M. Roesner has received project funding from Novartis and Almirall. C. Schlapbach has received honoraria as adviser or speaker for AbbVie, Almirall, BMS, Incyte, LEO Pharma, Lilly, Kiowa Kirin, Novartis, Pfizer, and Sanofi; and has received research funding from PPM Services A. Thorsti Møller Rønnstad has received research funding from the Department of Clinical Medicine, Copenhagen University, and the Kgl Hofbuntmager Aage Bangs Foundation. J. P. Thyssen has served as advisor for AbbVie, Almirall, Arena Pharmaceuticals, Coloplast, OM Pharma, Aslan Pharmaceuticals, Union Therapeutics, Eli Lilly, Pfizer, Regeneron, and Sanofi-Genzyme; has served as speaker for AbbVie, Almirall, Eli Lilly, Pfizer, Regeneron, and Sanofi Genzyme; and has received research grants from Pfizer, Regeneron, and Sanofi Genzyme; and has, since May 2023, been employed at LEO Pharma, where he holds stock options.

We thank the next-generation sequencing platform and the flow cytometry and cell sorting core facility of the Department of BioMedical Research, University of Bern, for performing the high-throughput sequencing experiments and FACS, respectively. The graphical abstract and Fig 3, *F,* were created with BioRender.com.

Key messages

- **T_H2 cells expressing the IL-18Rα are increased in both blood and lesional skin of AD patients compared to HD.**
- **IL-9 induces IL-18R expression on T_H2 cells through an IL-9R-JAK1/JAK3-STAT1 signaling pathway, facilitating IL-18–mediated secretion of IL-13 and IL-22.**
- **Neutralizing IL-18 downregulates pathogenic cytokine expression from T_H2 cells in lesional AD skin biopsy samples, suggesting IL-18 may be a potential therapeutic target for AD treatment.**

REFERENCES

1. Weidinger S, Beck LA, Bieber T, Kabashima K, Irvine AD. Atopic dermatitis. Nat Rev Dis Primers 2018;4:1.
2. Langan SM, Irvine AD, Weidinger S. Atopic dermatitis. Lancet 2020;396:345-60.
3. Kolkhir P, Akdis CA, Akdis M, Bachert C, Bieber T, Canonica GW, et al. Type 2 chronic inflammatory diseases: targets, therapies and unmet needs. Nat Rev Drug Discov 2023;22:743-67.
4. Zhang B, Roesner LM, Traidl S, Koeken V, Xu CJ, Werfel T, et al. Single-cell profiles reveal distinctive immune response in atopic dermatitis in contrast to psoriasis. Allergy 2023;78:439-53.
5. Roediger B, Schlapbach C. T cells in the skin: lymphoma and inflammatory skin disease. J Allergy Clin Immunol 2022;149:1172-84.
6. Reich K, Armstrong AW, Langley RG, Flavin S, Randazzo B, Li S, et al. Guselkumab versus secukinumab for the treatment of moderate-to-severe psoriasis (ECLIPSE): results from a phase 3, randomised controlled trial. Lancet 2019; 394:831-9.
7. Schnell A, Littman DR, Kuchroo VK. TH17 cell heterogeneity and its role in tissue inflammation. Nat Immunol 2023;24:19-29.
8. Lee JS, Tato CM, Joyce-Shaikh B, Gulen MF, Cayatte C, Chen Y, et al. Interleukin-23–independent IL-17 production regulates intestinal epithelial permeability. Immunity 2015;43:727-38.
9. Li J, Casanova JL, Puel A. Mucocutaneous IL-17 immunity in mice and humans: host defense vs excessive inflammation. Mucosal Immunol 2018;11:581-9.
10. Armstrong AW, Blauvelt A, Mrowietz U, Strober B, Gisondi P, Merola JF, et al. A practical guide to the management of oral candidiasis in patients with plaque psoriasis receiving treatments that target interleukin-17. Dermatol Ther (Heidelb) 2022;12:787-800.
11. Bertschi NL, Bazzini C, Schlapbach C. The concept of pathogenic T_H2 cells: Collegium Internationale Allergologicum update, 2021. Int Arch Allergy Immunol 2021;182:365-80.
12. Paternoster L, Standl M, Waage J, Baurecht H, Hotze M, Strachan DP, et al. Multi-ancestry genome-wide association study of 21,000 cases and 95,000 controls identifies new risk loci for atopic dermatitis. Nat Genet 2015;47:1449-56.

13. Ellinghaus D, Baurecht H, Esparza-Gordillo J, Rodriguez E, Matanovic A, Marenholz I, et al. High-density genotyping study identifies four new susceptibility loci for atopic dermatitis. Nat Genet 2013;45:808-12.
14. Sobczyk MK, Richardson TG, Zuber V, Min JL, Gaunt TR, Paternoster L, et al. Triangulating molecular evidence to prioritize candidate causal genes at established atopic dermatitis loci. J Invest Dermatol 2021;141:2620-9.
15. Halling AS, Rinnov MR, Ruge IF, Gerner T, Ravn NH, Knudgaard MH, et al. Skin TARC/CCL17 increase precedes the development of childhood atopic dermatitis. J Allergy Clin Immunol 2022;1550-7.
16. Andersson AM, Solberg J, Koch A, Skov L, Jakasa I, Kezic S, et al. Assessment of biomarkers in pediatric atopic dermatitis by tape strips and skin biopsies. Allergy 2022;77:1499-509.
17. Kaplanski G. Interleukin-18: biological properties and role in disease pathogenesis. Immunol Rev 2018;281:138-53.
18. Trzeciak M, Glen J, Bandurski T, Sokolowska-Wojdylo M, Wilkowska A, Roszkiewicz J. Relationship between serum levels of interleukin-18, IgE and disease severity in patients with atopic dermatitis. Clin Exp Dermatol 2011;36:728-32.
19. Renert-Yuval Y, Thyssen JP, Bissonnette R, Bieber T, Kabashima K, Hijnen D, et al. Biomarkers in atopic dermatitis—a review on behalf of the International Eczema Council. J Allergy Clin Immunol 2021;147:1174-90.e1.
20. Kezic S, O'Regan GM, Lutter R, Jakasa I, Koster ES, Saunders S, et al. Filaggrin loss-of-function mutations are associated with enhanced expression of IL-1 cytokines in the stratum corneum of patients with atopic dermatitis and in a murine model of filaggrin deficiency. J Allergy Clin Immunol 2012;129:1031-9.e1.
21. Sakai T, Hatano Y, Zhang W, Fujiwara S, Nishiyori R. Knockdown of either filaggrin or loricrin increases the productions of interleukin (IL)-1α, IL-8, IL-18 and granulocyte macrophage colony-stimulating factor in stratified human keratinocytes. J Dermatol Sci 2015;80:158-60.
22. Michaelidou M, Redhu D, Kumari V, Babina M, Worm M. IL-1α/β and IL-18 profiles and their impact on claudin-1, loricrin and filaggrin expression in patients with atopic dermatitis. J Eur Acad Dermatol Venereol 2023;37:e1141-3.
23. Chen JL, Niu XL, Gao YL, Ma L, Gao XH, Chen HD, et al. IL-18 knockout alleviates atopic dermatitis-like skin lesions induced by MC903 in a mouse model. Int J Mol Med 2020;46:880-8.
24. Konishi H, Tsutsui H, Murakami T, Yumikura-Futatsugi S, Yamanaka K, Tanaka M, et al. IL-18 contributes to the spontaneous development of atopic dermatitis-like inflammatory skin lesion independently of IgE/stat6 under specific pathogen-free conditions. Proc Natl Acad Sci U S A 2002;99:11340-5.
25. Vivier E, van de Pavert SA, Cooper MD, Belz GT. The evolution of innate lymphoid cells. Nat Immunol 2016;17:790-4.
26. Ricardo-Gonzalez RR, Van Dyken SJ, Schneider C, Lee J, Nussbaum JC, Liang HE, et al. Tissue signals imprint ILC2 identity with anticipatory function. Nat Immunol 2018;19:1093-9.
27. Naik SM, Cannon G, Burbach GJ, Singh SR, Swerlick RA, Wilcox JN, et al. Human keratinocytes constitutively express interleukin-18 and secrete biologically active interleukin-18 after treatment with pro-inflammatory mediators and dinitrochlorobenzene. J Invest Dermatol 1999;113:766-72.
28. Wang B, Feliciani C, Howell BG, Freed I, Cai Q, Watanabe H, et al. Contribution of Langerhans cell–derived IL-18 to contact hypersensitivity. J Immunol 2002;168:3303-8.
29. Bauernfried S, Hornung V. Human NLRP1: from the shadows to center stage. J Exp Med 2022;219:e20211405.
30. Wang X, Wang L, Wen X, Zhang L, Jiang X, He G. Interleukin-18 and IL-18BP in inflammatory dermatological diseases. Front Immunol 2023;14:955369.
31. Angkasekwinai P, Dong C. IL-9–producing T cells: potential players in allergy and cancer. Nat Rev Immunol 2021;21:37-48.
32. Micossé C, von Meyenn L, Steck O, Kipfer E, Adam C, Simillion C, et al. Human "T_H9" cells are a subpopulation of PPAR-γ^+ T_H2 cells. Sci Immunol 2019;4:eaat5943.
33. Bertschi NL, Steck O, Luther F, Bazzini C, von Meyenn L, Scharli S, et al. PPAR-γ regulates the effector function of human T helper 9 cells by promoting glycolysis. Nat Commun 2023;14:2471.
34. Clark RA, Schlapbach C. T_H9 cells in skin disorders. Semin Immunopathol 2017;39:47-54.
35. Möbus L, Rodriguez E, Harder I, Stolzl D, Boraczynski N, Gerdes S, et al. Atopic dermatitis displays stable and dynamic skin transcriptome signatures. J Allergy Clin Immunol 2021;147:213-23.
36. Ciprandi G, De Amici M, Giunta V, Marseglia A, Marseglia G. Serum interleukin-9 levels are associated with clinical severity in children with atopic dermatitis. Pediatr Dermatol 2013;30:222-5.
37. Eyerich S, Eyerich K, Pennino D, Carbone T, Nasorri F, Pallotta S, et al. Th22 cells represent a distinct human T cell subset involved in epidermal immunity and remodeling. J Clin Invest 2009;119:3573-85.
38. Reynolds G, Vegh P, Fletcher J, Poyner EFM, Stephenson E, Goh I, et al. Developmental cell programs are co-opted in inflammatory skin disease. Science 2021;371:eaba6500.
39. Bangert C, Rindler K, Krausgruber T, Alkon N, Thaler FM, Kurz H, et al. Persistence of mature dendritic cells, T_H2A, and Tc2 cells characterize clinically resolved atopic dermatitis under IL-4Ralpha blockade. Sci Immunol 2021;6:eabe2749.
40. Alkon N, Assen FP, Arnoldner T, Bauer WM, Medjimorec MA, Shaw LE, et al. Single-cell RNA sequencing defines disease-specific differences between chronic nodular prurigo and atopic dermatitis. J Allergy Clin Immunol 2023;152:420-35.
41. Ma F, Gharaee-Kermani M, Tsoi LC, Plazyo O, Chaskar P, Harms P, et al. Single-cell profiling of prurigo nodularis demonstrates immune–stromal crosstalk driving profibrotic responses and reversal with nemolizumab. J Allergy Clin Immunol 2024;153:146-60.
42. Kim D, Langmead B, Salzberg SL. HISAT: a fast spliced aligner with low memory requirements. Nat Methods 2015;12:357-60.
43. Anders S, Pyl PT, Huber W. HTSeq—a Python framework to work with high-throughput sequencing data. Bioinformatics 2015;31:166-9.
44. Love MI, Huber W, Anders S. Moderated estimation of fold change and dispersion for RNA-Seq data with DESeq2. Genome Biol 2014;15:550.
45. Butler A, Hoffman P, Smibert P, Papalexi E, Satija R. Integrating single-cell transcriptomic data across different conditions, technologies, and species. Nat Biotechnol 2018;36:411-20.
46. Schäbitz A, Hillig C, Mubarak M, Jargosch M, Farnoud A, Scala E, et al. Spatial transcriptomics landscape of lesions from non-communicable inflammatory skin diseases. Nat Commun 2022;13:7729.
47. Wambre E, Bajzik V, DeLong JH, O'Brien K, Nguyen QA, Speake C, et al. A phenotypically and functionally distinct human T_H2 cell subpopulation is associated with allergic disorders. Sci Transl Med 2017;9:eaam9171.
48. Bonnal RJ, Ranzani V, Arrigoni A, Curti S, Panzeri I, Gruarin P, et al. *De novo* transcriptome profiling of highly purified human lymphocytes primary cells. Sci Data 2015;2:150051.
49. Ivashkiv LB, Donlin LT. Regulation of type I interferon responses. Nat Rev Immunol 2014;14:36-49.
50. Yin T, Yang L, Yang YC. Tyrosine phosphorylation and activation of JAK family tyrosine kinases by interleukin-9 in MO7E cells. Blood 1995;85:3101-6.
51. Silverberg JI, Guttman-Yassky E, Thaci D, Irvine AD, Stein Gold L, Blauvelt A, et al. Two phase 3 trials of lebrikizumab for moderate-to-severe atopic dermatitis. N Engl J Med 2023;388:1080-91.
52. Wollenberg A, Howell MD, Guttman-Yassky E, Silverberg JI, Kell C, Ranade K, et al. Treatment of atopic dermatitis with tralokinumab, an anti–IL-13 mAb. J Allergy Clin Immunol 2019;143:135-41.
53. Ackerman L, Acloque G, Bacchelli S, Schwartz H, Feinstein BJ, La Stella P, et al. IRAK4 degrader in hidradenitis suppurativa and atopic dermatitis: a phase 1 trial. Nat Med 2023;3127-36.
54. International Eczema Council (IEC). Target lesion severity score (TLSS) for the assessment of atopic dermatitis (AD). n.d. Available at: https://www.ieclearning.com.
55. Thijs J, Krastev T, Weidinger S, Buckens CF, de Bruin-Weller M, Bruijnzeel-Koomen C, et al. Biomarkers for atopic dermatitis: a systematic review and meta-analysis. Curr Opin Allergy Clin Immunol 2015;15:453-60.
56. Hijnen D, De Bruin-Weller M, Oosting B, Lebre C, De Jong E, Bruijnzeel-Koomen C, et al. Serum thymus and activation-regulated chemokine (TARC) and cutaneous T cell– attracting chemokine (CTACK) levels in allergic diseases: TARC and CTACK are disease-specific markers for atopic dermatitis. J Allergy Clin Immunol 2004;113:334-40.
57. Nakanishi K, Yoshimoto T, Tsutsui H, Okamura H. Interleukin-18 regulates both Th1 and Th2 responses. Annu Rev Immunol 2001;19:423-74.
58. Vaher H, Kingo K, Kolberg P, Pook M, Raam L, Laanesoo A, et al. Skin colonization with *S aureus* can lead to increased NLRP1 inflammasome activation in patients with atopic dermatitis. J Invest Dermatol 2023;143:1268-78.e8.
59. Fyhrquist N, Muirhead G, Prast-Nielsen S, Jeanmougin M, Olah P, Skoog T, et al. Microbe–host interplay in atopic dermatitis and psoriasis. Nat Commun 2019;10:4703.
60. Shi X, Sun Q, Hou Y, Zeng H, Cao Y, Dong M, et al. Recognition and maturation of IL-18 by caspase-4 noncanonical inflammasome. Nature 2023;442-50.
61. Paller AS, Kong HH, Seed P, Naik S, Scharschmidt TC, Gallo RL, et al. The microbiome in patients with atopic dermatitis. J Allergy Clin Immunol 2019;143:26-35.
62. Simpson EL, Parnes JR, She D, Crouch S, Rees W, Mo M, et al. Tezepelumab, an anti-thymic stromal lymphopoietin monoclonal antibody, in the treatment of moderate to severe atopic dermatitis: a randomized phase 2a clinical trial. J Am Acad Dermatol 2019;80:1013-21.
63. Agnihotri G, Lio PA. Revisiting therapies for atopic dermatitis that failed clinical trials. Clin Drug Investig 2020;40:421-31.

64. Schuler CFt, Gudjonsson JE. IL-33 antagonism does not improve chronic atopic dermatitis: what can we learn? J Allergy Clin Immunol 2022;150:1410-1.
65. Maurer M, Cheung DS, Theess W, Yang X, Dolton M, Guttman A, et al. Phase 2 randomized clinical trial of astegolimab in patients with moderate to severe atopic dermatitis. J Allergy Clin Immunol 2022;150:1517-24.
66. Lavazais S, Jargosch M, Dupont S, Labeguere F, Menet C, Jagerschmidt C, et al. IRAK4 inhibition dampens pathogenic processes driving inflammatory skin diseases. Sci Transl Med 2023;15:eabj3289.
67. Yoshimoto T, Mizutani H, Tsutsui H, Noben-Trauth N, Yamanaka K, Tanaka M, et al. IL-18 induction of IgE: dependence on $CD4^+$ T cells, IL-4 and STAT6. Nat Immunol 2000;1:132-7.
68. Schlapbach C, Gehad A, Yang C, Watanabe R, Guenova E, Teague JE, et al. Human T_H9 cells are skin-tropic and have autocrine and paracrine proinflammatory capacity. Sci Transl Med 2014;6:219ra8.
69. Klicznik MM, Morawski PA, Hollbacher B, Varkhande SR, Motley SJ, Kuri-Cervantes L, et al. Human $CD4^+CD103^+$ cutaneous resident memory T cells are found in the circulation of healthy individuals. Sci Immunol 2019;4:eaav8995.
70. Son A, Meylan F, Gomez-Rodriguez J, Kaul Z, Sylvester M, Falduto GH, et al. Dynamic chromatin accessibility licenses STAT5- and STAT6-dependent innate-like function of T_H9 cells to promote allergic inflammation. Nat Immunol 2023;24:1036-48.
71. Bauer JH, Liu KD, You Y, Lai SY, Goldsmith MA. Heteromerization of the gammac chain with the interleukin-9 receptor alpha subunit leads to STAT activation and prevention of apoptosis. J Biol Chem 1998;273:9255-60.
72. Kalbasi A, Siurala M, Su LL, Tariveranmoshabad M, Picton LK, Ravikumar P, et al. Potentiating adoptive cell therapy using synthetic IL-9 receptors. Nature 2022;607:360-5.
73. Schlapbach C, Conrad C. TYK-ing all the boxes in psoriasis. J Allergy Clin Immunol 2022;149:1936-9.
74. Chou PH, Luo CK, Wali N, Lin WY, Ng SK, Wang CH, et al. A chemical probe inhibitor targeting STAT1 restricts cancer stem cell traits and angiogenesis in colorectal cancer. J Biomed Sci 2022;29:20.
75. Bai L, Zhou H, Xu R, Zhao Y, Chinnaswamy K, McEachern D, et al. A potent and selective small-molecule degrader of STAT3 achieves complete tumor regression *in vivo*. Cancer Cell 2019;36:498-511.e17.
76. Clark RA, Chong B, Mirchandani N, Brinster NK, Yamanaka K, Dowgiert RK, et al. The vast majority of CLA^+ T cells are resident in normal skin. J Immunol 2006;176:4431-9.

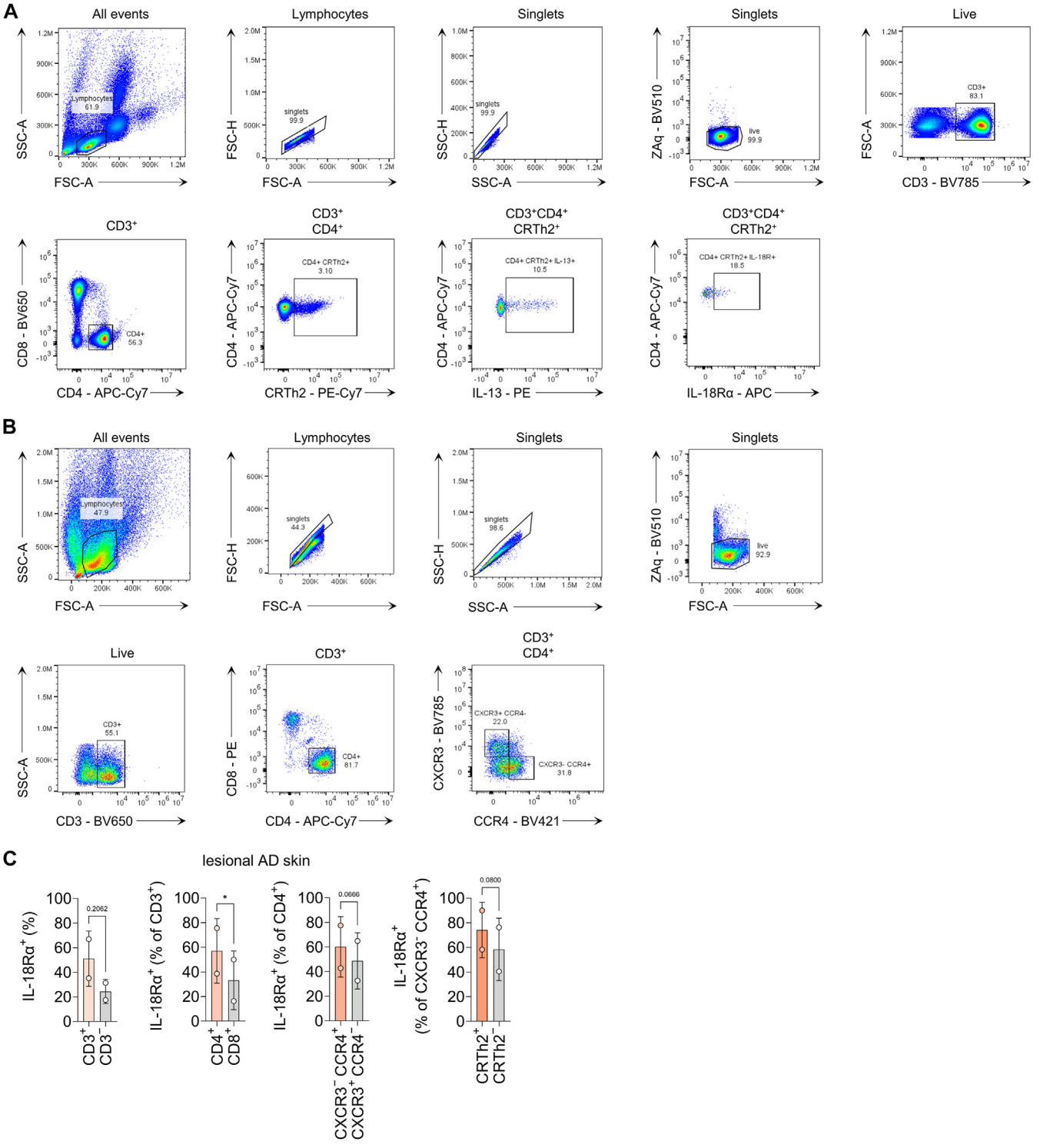

FIG E1. Gating strategies for flow cytometry and cell sorting. (A) Gating strategy for identification of IL-13 secretion and IL-18R expression in CRT_H2^+ T_H cells in PBMCs of AD patients and HD by flow cytometry for Fig 1, *D*, Fig 2, *G*, and Fig 4, *B* and *C*. **(B)** Gating strategy for detection of IL-18R–expressing $CXCR3^-CCR4^+CRT_H2^+CD4^+$ T cells in lesional AD skin for Fig 1, *E*. **(C)** IL-18R expression of $CD3^+/CD3^-$, $CD4^+/CD8^+$, $CXCR3^-CCR4^+/CXCR3^+CCR4^-$, and$CXCR3^-CCR4^+CRT_H2^+/CXCR3^-CCR4^+CRT_H2^-$ cells from lesional AD skin for Fig 1, *E*.

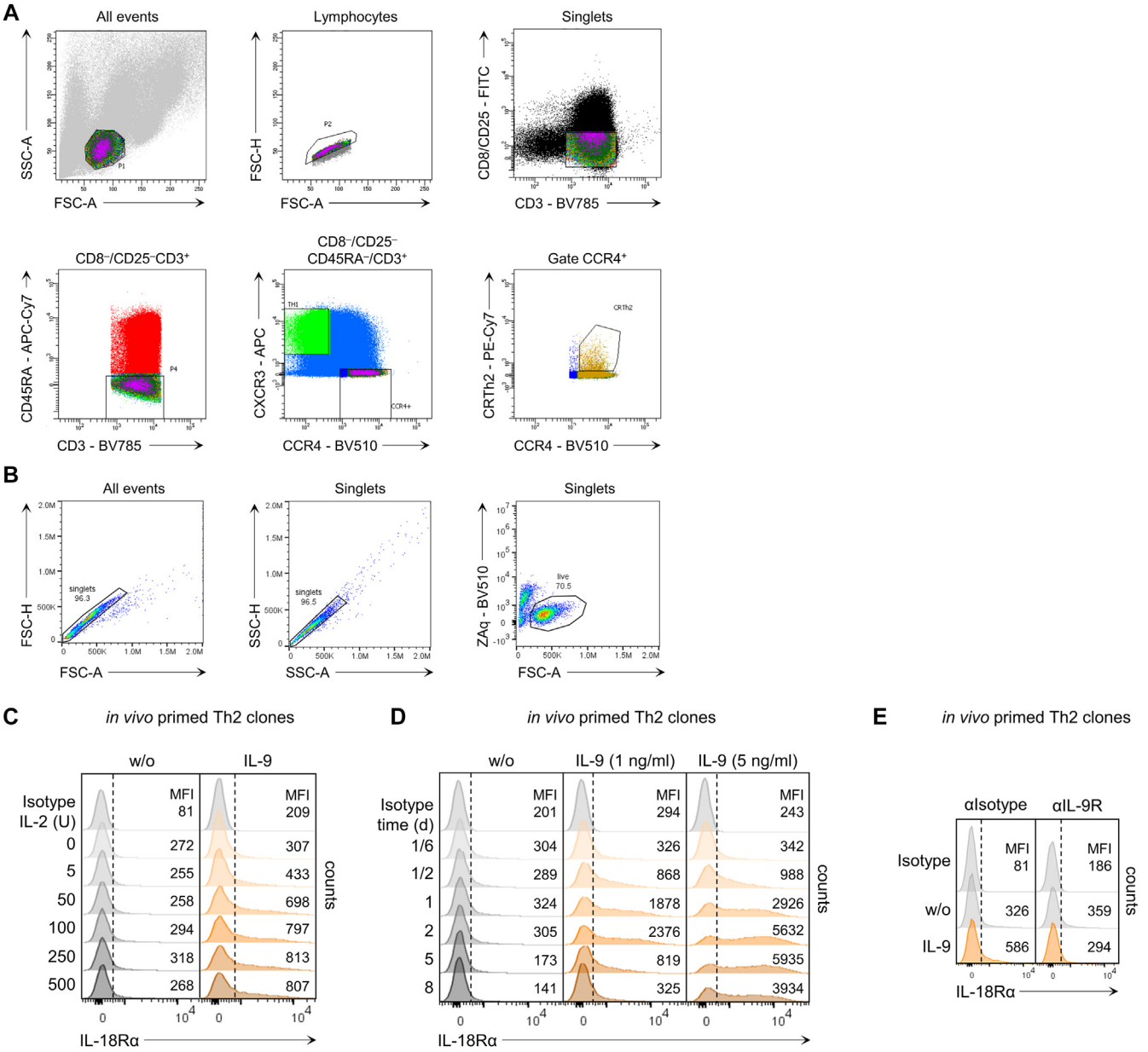

FIG E2. Gating strategies for flow cytometry. (A) Gating strategy for T_H cell subset clones sorted for Fig 2, *A-D,* and Fig 3, *A-D.* $CD4^+$ T cells were isolated from PBMCs of HD and stained for subsequent sorting of T_H cell subset. *In vivo* primed T_H2 clones were generated according to chemokine receptor expression $CXCR3^-CCR4^+CRT_H2^+$ from $CD45RA^-CD25^-CD8^-CD3^+$ cells. **(B)** Gating strategy for Fig 2, *A-D,* Fig 3, *B-D,* and Fig 4, *F* and *G (left),* of *in vitro* primed T_H2 cells or FACS *in vivo* primed T_H2 clones. Cells were gated based on forward scatter height (FSC-H) and forward scatter area (FSC-A), as well as side scatter height (SSC-H) and side scatter area (SSC-A) to ensure singlets. Live cells were then selected by excluding zombie aqua (ZAq)-positive cells. Finally, receptor expression or phosphorylation of targets of interest were analyzed in selected live cells. **(C)** Representative histogram plots of 1 donor displaying IL-18R expression levels in *in vivo* primed T_H2 clones on different IL-2 concentrations, in presence or absence of IL-9 for Fig 2, *B.* **(D)** Representative histogram plots of 1 donor displaying time course of IL-18R expression levels in *in vivo* primed T_H2 clones cultured in IL-2 and different concentrations of IL-9 for Fig 2, *C.* **(E)** Representative histogram plots of 1 donor displaying IL-18R expression in *in vivo* primed T_H2 clones on IL-9R blockade or isotype control, in presence or absence of IL-9 for Fig 2, *D.*

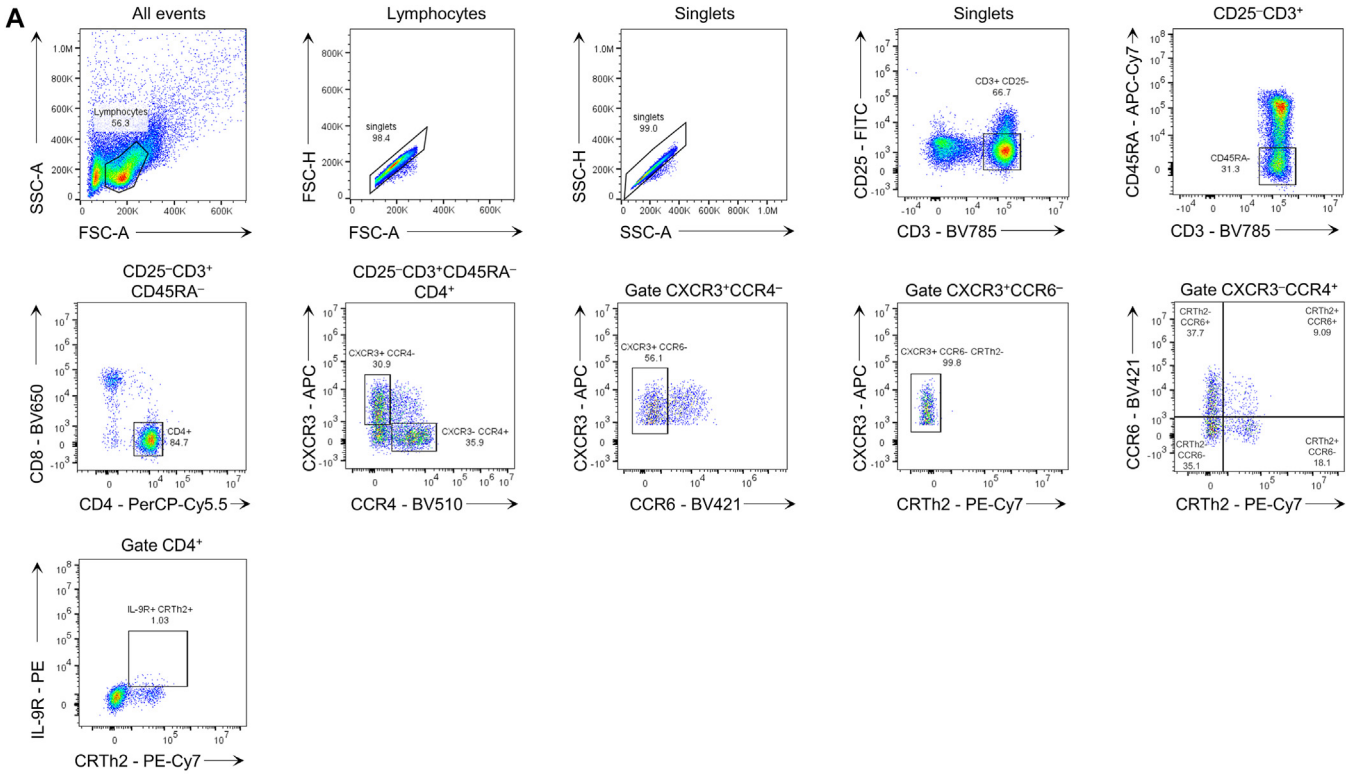

FIG E3. Gating strategies for flow cytometry. (A and B) Gating strategy for assessing IL-9R-expressing CRT_H2^+ memory $CD4^+$ T cells for Fig 2, *E (A),* and representative histogram plots of 1 donor displaying IL-9R expression in memory $CD4^+$ T-cell subsets for Fig 2, *F (B),* in PBMCs of AD patients by flow cytometry. **(C)** IFN-α2 expression measured in cell culture supernatant of *in vivo* primed T_H2 clones incubated with IL-9 for 48 hours. **(D)** Western blot of pJAK1 *(left)*, pJAK3 *(middle),* and pTYK2 *(right)* in *in vivo* primed T_H2 clones on IL-9 stimulation for 5 minutes.

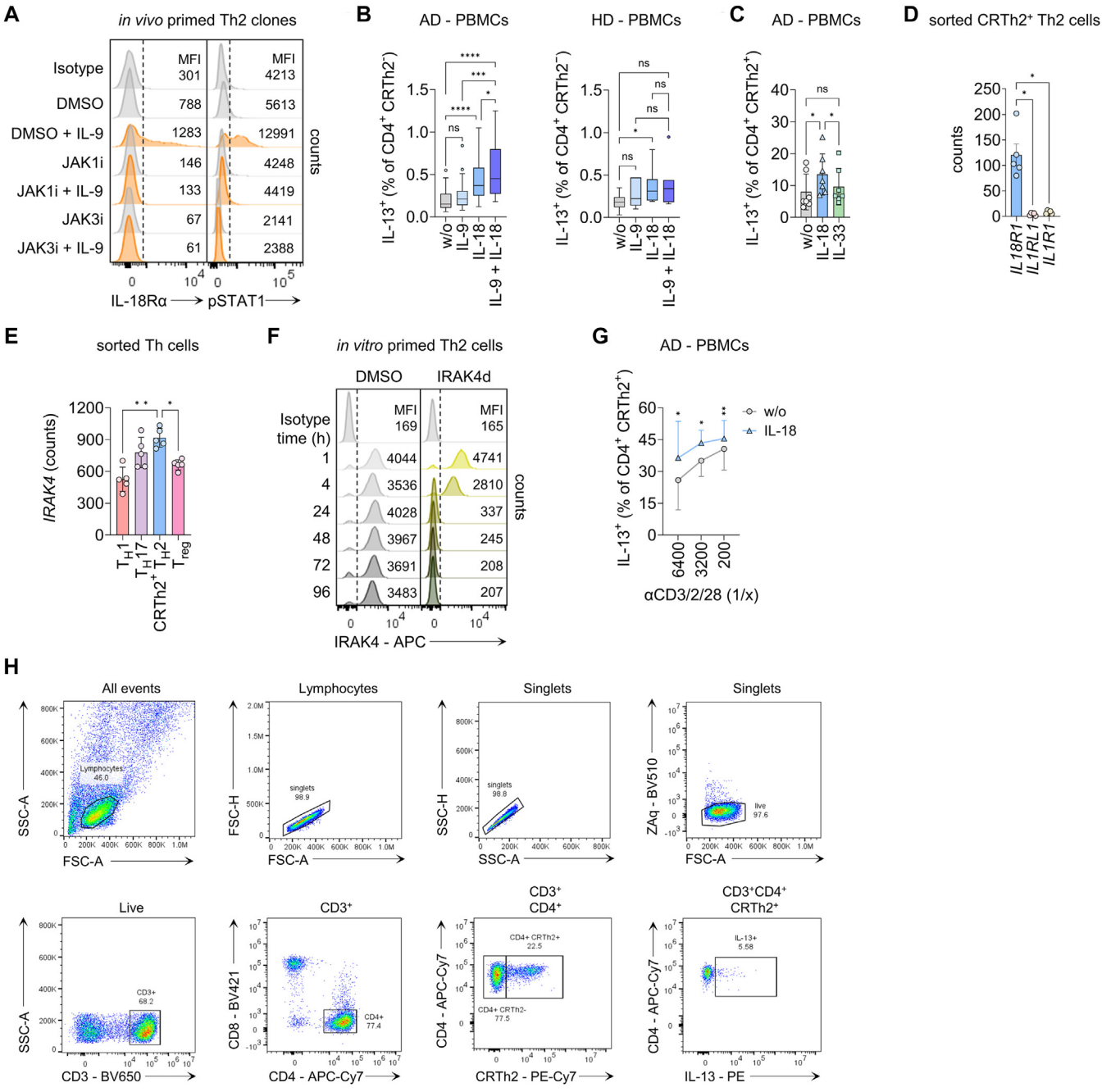

FIG E4. Gating strategies for flow cytometry. (A) Representative histogram plots of 1 donor displaying IL-18R expression and pSTAT1 induction in *in vivo* primed T_H2 clones on IL-9 stimulation in presence or absence of JAK1 inhibitor (JAK1i) upadacitinib and JAK3 inhibitor (JAK3i) ritlecitinib for Fig 3, *D*. **(B)** IL-13 secretion of $CD4^+$ CRT_H2^- cells of PBMCs from AD donors incubated with IL-9 and/or IL-18 for 16 hours, assessed by IL-13 Secretion Assay (Miltenyi Biotec) by flow cytometry. **(C)** IL-13 secretion of $CD4^+$ CRT_H2^+ cells of PBMCs from AD donors incubated with IL-18 and IL-33 for 16 hours, assessed by IL-13 Secretion Assay (Miltenyi Biotec) by flow cytometry. **(D)** *IL18R1, IL1RL1,* and *IL1R1* expression in sorted CRT_H2^+ T_H2 cells from HD assessed by RNA-Seq. **(E)** *IRAK4* expression in sorted T_H cell subsets from HD assessed by RNA-Seq. **(F)** Representative histogram plots of 1 donor displaying time course of IRAK4 expression levels in *in vitro* primed T_H2 cells cultured in presence or absence of IRAK4 degrader (IRAK4d) KT-474 (SAR444656) for Fig 3, *G*. **(G)** IL-13 secretion of $CD4^+$ CRT_H2^+ cells of PBMCs from AD donors incubated with different concentrations of αCD3/2/28 and/or IL-18 for 16 hours, assessed by IL-13 Secretion Assay (Miltenyi Biotec) by flow cytometry. **(H)** Gating strategy for identification of egressed IL-13–secreting CRT_H2^+ and CRT_H2^- $CD4^+$ T cells from lesional AD skin measured by IL-13 Secretion Assay (Miltenyi Biotec) by flow cytometry for Fig 5, C.

TABLE E1. Baseline demographics for Fig 5, *B* and *C*

Characteristic	Value (N = 4)
Age (years), median (IQR)	54 (37.25-69.5)
Female	25 (1)
EASI*	
Mild	0
Moderate	50 (2)
Severe	50 (2)
Atopic comorbidities	75 (3)

Data are presented as % (nos.) unless otherwise indicated.
EASI, Eczema Area Severity Index; *IQR,* interquartile range.
*Mild AD was defined as EASI index score 0-7; moderate AD, 7.1-20.9; and severe AD, >21.

TABLE E2. Baseline demographics for Fig 5, *D*

Characteristic	Value (N = 41)
Age (years), median (IQR)	24 (22-25)
Female	63.41 (26)
TLSS, mean ± SD	2.95 ± 1.58
EASI	
Mild	63.41 (26)
Moderate	24.39 (10)
Severe	12.20 (5)
Atopic comorbidities	58.54 (24)

Data are presented as % (nos.) unless otherwise indicated.
EASI, Eczema Area Severity Index; *IQR,* interquartile range; *TLSS,* target lesion severity score.
Mild AD was defined as EASI index score 0-7; moderate AD, 7.1-20.9; and severe AD, >21.

TABLE E3. Antibodies used

Characteristic	Antibody	Clone	Conjugation	Company (catalog no.)	Dilution
Flow cytometry—surface staining	Mouse anti-human CXCR3, mAb	G025H7	AF647	BioLegend (353712)	1:60
		G025H7	BV785	BioLegend (353738)	1:100
	Mouse anti-human CD45RA, mAb	HI100	APC-Cy7	BioLegend (304127)	1:200
	Mouse anti-human CD8, mAb	RPA-T8	AF488	BioLegend (301021)	1:100
		RPA-T8	PE	BD Biosciences (555367)	1:400
		SK1	BV421	BioLegend (344747)	1:400
		RPA-T8	BV650	BioLegend (301042)	1:400
	Mouse anti-human CD25, mAb	BC96	FITC	BioLegend (302603)	1:100
	Mouse anti-human CCR8, mAb	L263G8	PE	BioLegend (360604)	1:60
	Mouse anti-human CCR4, mAb	L291H4	PE-Cy7	BioLegend (359410)	1:60
		L291H4	BV421	BioLegend (359414)	1:200
		L291H4	BV510	BioLegend (359416)	1:100
	Mouse anti-human CCR6, mAb	G034E3	PerCP-Cy5.5	BioLegend (353406)	1:60
		G034E3	BV421	BioLegend (353407)	1:100
	Mouse anti-human CD3, mAb	OKT3	BV650	BioLegend (317324)	1:200
		OKT3	BV785	BioLegend (317330)	1:400
	Mouse anti-human CD4, mAb	OKT4	APC-Cy7	BioLegend (317417)	1:400
		OKT4	PerCP-Cy5.5	BioLegend (317427)	1:400
	Mouse anti-human IL-9R, mAb	AH9R7	PE	BioLegend (310404)	1:200
	Mouse anti-human IgG_2b, mAb	MG2b-57	PE	BioLegend (401207)	1:200
	Mouse anti-human IL-18Rα, mAb	H44	APC	BioLegend (313813)	1:200
	Mouse anti-human IgG_1, mAb	MOPC-21	APC	BioLegend (400119)	1:200
	Mouse anti-human CRT_H2, mAb	BM16	PE-Cy7	BioLegend (350117)	1:50
	Zombie Aqua		BV510	BioLegend (423101)	1:800
Flow cytometry—intracellular staining	Rabbit anti-human phospho-STAT1 (Tyr701), mAb	58D6	AF488	Cell Signaling (9174)	1:200
	Rabbit anti-human IgG, mAb	MOPC-21	AF488	Cell Signaling (4340)	1:600
	Mouse anti-human phospho-STAT3 (Tyr705), mAb	13A3-1	BV421	BioLegend (651009)	1:200
	Mouse anti-human IgG_1, mAb	MOPC-21	BV421	BioLegend (400158)	1:400
	Mouse anti-human phospho-STAT4 (Tyr693), mAb	4LURPIE	PE	Thermo Fisher (12-9044-41)	1:200
	Mouse anti-human IgG_1, mAb	MOPC-21	PE	BioLegend (400111)	1:1600
	Mouse anti-human phospho-STAT5 (Tyr694), mAb	A17016B.Rec	PE-Cy7	BioLegend (936907)	1:200
	Mouse anti-human IgG_1, mAb	MOPC-21	PE-Cy7	BioLegend (400125)	1:800
	Mouse anti-human phospho-STAT6 (Tyr641), mAb	A15137E	APC	BioLegend (686017)	1:200
	Rabbit anti-human phospho-NF-κB p65 (Ser536), mAb	93H1	PE	Cell Signaling (5733)	1:200
	Rabbit anti-human phospho-*c*-Jun (Ser73), mAb	D47G9	PE	Cell Signaling (8752)	1:100
	Human anti-human IRAK4, mAb	REA462	APC	Miltenyi Biotec (130-120-307)	1:200
	Human anti-human IgG_1, mAb	REA293	APC	Miltenyi Biotec (130-120-709)	1:200
Western blot analysis	Rabbit anti-human phospho-JAK1, mAb	D7N4Z	Unconjugated	Cell Signaling (74129)	1:1000
	Rabbit anti-human phospho-JAK3, mAb	D44E3	Unconjugated	Cell Signaling (5031)	1:1000
	Rabbit anti-human phospho-TYK2, mAb	D7T8A	Unconjugated	Cell Signaling (68790)	1:1000
	Mouse anti-human F-actin, mAb	ACTN05	Unconjugated	Invitrogen (MA5-11869)	1:6000
	Goat anti-rabbit IgG, pAb		HRP	Thermo Fisher Scientific (31462)	1:5000
	Goat anti-mouse IgG, pAb		HRP	Thermo Fisher Scientific (G21040)	1:5000

TABLE E4. RT-qPCR primers

Gene transcript	Gene	Species	TaqMan primer	Company
IL-13	*IL13*	Human	Hs00174379_m1	Thermo Fisher Scientific
HPRT1	*HPRT1*	Human	Hs99999909_m1	Thermo Fisher Scientific

TABLE E5. Recombinant proteins and chemicals used

Characteristic	Name	Format	Company (catalog no.)	Final concentration
Recombinant proteins	Recombinant human IL-2	Purified	Hoffmann-La Roche	5/50/100/250/500 U/mL
	Recombinant human IL-4	Purified	BioLegend (574006)	50 ng/mL
	Recombinant human IL-7	Purified	BioLegend (581904)	20 μg/mL
	Recombinant human IL-9	Purified	BioLegend (594404)	1/5 ng/mL
	Recombinant human IL-15	Purified	BioLegend (570304)	100 ng/mL
	Recombinant human IL-18	Purified	BioLegend (592104)	100 ng/mL
	Recombinant human IL-21	Purified	BioLegend (571204)	100 ng/mL
	Recombinant human IL-17E/IL-25	Purified	BioLegend (598904)	1 μg/mL
	Recombinant human IL-33	Purified	BioLegend (581802)	50 ng/mL
	Recombinant human IFN-α2	Purified	BioLegend (592704)	5.4 ng/mL
	Recombinant human TGF-β1	Purified	R&D Systems (240-B-010/CF)	5 ng/mL
	Recombinant human TSLP	Purified	BioLegend (582404)	50 ng/mL
Chemicals	Anti-human CD129 (IL-9R), mAb	LEAF purified	BioLegend (310408)	10 μg/mL
	Anti-human mouse IgG_2b, κ, mAb	LEAF purified	BioLegend (400339)	10 μg/mL
	DMSO	Purified	Sigma-Aldrich (D8418)	50/1000 nmol
	Upadacitinib (ABT-494)	Purified	Selleckchem (S8162)	50 nmol
	Ritlecitinib (PF-06651600)	Purified	Selleckchem (S8538)	100 nmol
	KT-474/KYM-001 (SAR444656)	Purified	LubioScience (HY-145483)	1 μmol
	Recombinant human IL-18BP-Fc chimera	Purified	BioLegend (789804)	1.25 μg/mL